



Tractostorm 2: Optimizing tractography dissection reproducibility with segmentation protocol dissemination

Francois Rheault, Kurt Schilling, Alex Valcourt-Caron, Antoine Théberge, Charles Poirier, Gabrielle Grenier, Guido Guberman, John Begnoche, Jon Haitz Legarreta, Leon Cai, et al.

► To cite this version:

Francois Rheault, Kurt Schilling, Alex Valcourt-Caron, Antoine Théberge, Charles Poirier, et al.. Tractostorm 2: Optimizing tractography dissection reproducibility with segmentation protocol dissemination. Human Brain Mapping, 2022, 43 (7), pp.2134-2147. <10.1002/hbm.25777>. <hal-03781904>

HAL Id: hal-03781904

<https://hal.science/hal-03781904v1>

Submitted on 20 Sep 2022

HAL is a multi-disciplinary open access archive for the deposit and dissemination of scientific research documents, whether they are published or not. The documents may come from teaching and research institutions in France or abroad, or from public or private research centers.

L'archive ouverte pluridisciplinaire **HAL**, est destinée au dépôt et à la diffusion de documents scientifiques de niveau recherche, publiés ou non, émanant des établissements d'enseignement et de recherche français ou étrangers, des laboratoires publics ou privés.









HAL Authorization

RESEARCH ARTICLE

WILEY

Tractostorm 2: Optimizing tractography dissection reproducibility with segmentation protocol dissemination

Francois Rheault¹  | Kurt G. Schilling^{2,3} | Alex Valcourt-Caron⁴ |
 Antoine Théberge^{4,5} | Charles Poirier⁴ | Gabrielle Grenier⁴ |
 Guido I. Guberman⁶  | John Begnoche⁷ | Jon Haitz Legarreta^{4,5} | Leon Y. Cai⁸ |
 Maggie Roy⁹ | Manon Edde⁴ | Marco Perez Caceres¹⁰ | Mario Ocampo-Pineda¹¹ |
 Noor Al-Sharif¹² | Philippe Karan⁴ | Pietro Bontempi¹³ | Sami Obaid^{4,14}  |
 Sara Bosticardo¹¹ | Simona Schiavi¹¹  | Viljami Sairanen¹¹ |
 Alessandro Daducci¹¹ | Laurie E. Cutting¹⁵  | Laurent Petit¹⁶  |
 Maxime Descoteaux⁴ | Bennett A. Landman^{1,2,3,17}

¹Electrical and Computer Engineering, Vanderbilt University, Nashville, Tennessee, USA

²Vanderbilt University Institute of Imaging, Nashville, Tennessee, USA

³Department of Radiology and Radiological Science, Vanderbilt University Medical Center, Nashville, Tennessee, USA

⁴Sherbrooke Connectivity Imaging Laboratory (SCIL), Département d'Informatique, Université de Sherbrooke, Sherbrooke, Québec, Canada

⁵Videos and Images Theory and Analytics Laboratory (VITAL), Département d'Informatique, Université de Sherbrooke, Sherbrooke, Québec, Canada

⁶Department of Neurology and Neurosurgery, Faculty of Medicine, McGill University, Montreal, Québec, Canada

⁷The Center for Cognitive Medicine, Department of Psychiatry, Vanderbilt University Medical Center, Nashville, Tennessee, USA

⁸Department of Biomedical Engineering, Vanderbilt University, Nashville, Tennessee, USA

⁹Research Center on Aging, Université de Sherbrooke, Sherbrooke, Québec, Canada

¹⁰Département de Radiologie Diagnostique, Université de Sherbrooke, Sherbrooke, Québec, Canada

¹¹BABA Center, Pediatric Research Center, Department of Clinical Neurophysiology, Children's Hospital, Helsinki University Hospital and University of Helsinki, Helsinki, Finland

¹²McGill Centre for Integrative Neuroscience (MCIN), McGill University, Montreal, Québec, Canada

¹³Department of Neurosciences, Biomedicine and Movement Sciences, University of Verona, Verona, Italy

¹⁴University of Montreal, Health Center Research Center, Montreal, Canada

¹⁵Vanderbilt Kennedy Center, Vanderbilt University Medical Center, Nashville, Tennessee, USA

¹⁶Groupe d'imagerie neurofonctionnelle, CNRS, CEA, IMN, University of Bordeaux, Bordeaux, France

¹⁷Computer Science, Vanderbilt University, Nashville, Tennessee, USA

Correspondence

Francois Rheault, Electrical and Computer Engineering, Vanderbilt University, Nashville, TN 37235.

Email: francois.rheault@vanderbilt.edu

Funding information

National Center for Research Resources, Grant/Award Number: UL1 RR024975-01; National Institute of Child Health and Human

Abstract

The segmentation of brain structures is a key component of many neuroimaging studies. Consistent anatomical definitions are crucial to ensure consensus on the position and shape of brain structures, but segmentations are prone to variation in their interpretation and execution. White-matter (WM) pathways are global structures of the brain defined by local landmarks, which leads to anatomical definitions being difficult

This is an open access article under the terms of the Creative Commons Attribution-NonCommercial License, which permits use, distribution and reproduction in any medium, provided the original work is properly cited and is not used for commercial purposes.

© 2022 The Authors. *Human Brain Mapping* published by Wiley Periodicals LLC.

Development, Grant/Award Number: P50HD103537; American NATIONAL INSTITUTE Of HEALTH, Grant/Award Numbers: R01EB017230, T32EB001628; ViSE/VICTR, Grant/Award Number: VR3029; Fonds de Recherche du Québec - Santé; Savoy Foundation; Emil Aaltonen Foundation; Brain Research Foundation; NIH, Grant/Award Number: 5T32GM007347

to convey, learn, or teach. Moreover, the complex shape of WM pathways and their representation using tractography (streamlines) make the design and evaluation of dissection protocols difficult and time-consuming. The first iteration of Tractostorm quantified the variability of a pyramidal tract dissection protocol and compared results between experts in neuroanatomy and nonexperts. Despite *virtual dissection* being used for decades, in-depth investigations of how learning or practicing such protocols impact dissection results are nonexistent. To begin to fill the gap, we evaluate an online educational tractography course and investigate the impact learning and practicing a dissection protocol has on interrater (groupwise) reproducibility. To generate the required data to quantify reproducibility across raters and time, 20 independent raters performed dissections of three bundles of interest on five Human Connectome Project subjects, each with four timepoints. Our investigation shows that the dissection protocol in conjunction with an online course achieves a high level of reproducibility (between 0.85 and 0.90 for the voxel-based Dice score) for the three bundles of interest and remains stable over time (repetition of the protocol). Suggesting that once raters are familiar with the software and tasks at hand, their interpretation and execution at the group level do not drastically vary. When compared to previous work that used a different method of communication for the protocol, our results show that incorporating a virtual educational session increased reproducibility. Insights from this work may be used to improve the future design of WM pathway dissection protocols and to further inform neuroanatomical definitions.

KEYWORDS

diffusion MRI, reproducibility, segmentation, tractography, virtual dissection, WM pathways

1 | INTRODUCTION

Effectively conveying information in a research setting is challenging. It is common to expect researchers to quickly understand complex information or to be able to fill in the gaps if the information is missing. When dealing with intricate tasks or software, this premise often leads to inefficient communication. For example, diffusion tractography is used to study the connections of the brain. A chosen protocol or method must be reproducible to facilitate studies of the white-matter (WM) pathways of the brain. Teaching and conveying a protocol involves describing both complex anatomy and software usage. In our previous work (Rheault et al., 2020), we introduced a pyramidal tract (PYT) dissection protocol inspired by (Chenot et al., 2019) and evaluated the performance of collaborators executing the instructions. Collaborators were split into two groups: Experts with advanced knowledge in neuroanatomy and nonexperts with only basic/no knowledge in neuroanatomy. Tractostorm (V1) showed experts and nonexperts had similar levels of variability (between 0.60 and 0.65 for the voxel-based Dice score) with a large deviation for the average.

In this work, we evaluate the efficacy of teaching an online education session for a WM dissection protocol. The purpose of this study is to help improve the future design of WM pathway

dissection protocols and to further inform neuroanatomical definitions by evaluating quality improvement data from a conducted course. This is a step toward creating standardized definitions and improving the way they are taught. Expertise in bundles reproducibility analysis from the mentioned prior work allows us to expand the current analysis into WM pathways spatial agreement. In addition to the original protocol (Rheault, De Benedictis et al., 2020, which only included PYT), we add two bundles (the arcuate fasciculus [AF] and body of the corpus callosum [CC]) to the project. The investigation of the efficacy of teaching an online course (as opposed to basing learning only on written instructions) aims to help to understand the complexity of anatomical and software descriptions and assess where difficulties are and where clarifications could be needed.

Magnetic resonance imaging (MRI) has become the tool of choice for the in vivo investigation of the brain in neuroimaging studies due to its high resolution and variety of available contrasts. MRI has become the gold standard for manual and automatic segmentation of cerebral structures in the hope of finding relevant biomarkers (Boccardi et al., 2011; Fennema-Notestine et al., 2009; Pagnozzi, Conti, Calderoni, Fripp, & Rose, 2018). However, this quest highlighted the heterogeneity of anatomical definitions (Frisoni et al., 2015; Gasperini et al., 2001; Rosario et al., 2011; Visser et al., 2019).

Diffusion MRI, and more specifically tractography, specializes in the virtual reconstruction of structural connectivity of the brain (Griffa, Baumann, Thiran, & Hagmann, 2013; Hagmann et al., 2008; Jones, Simmons, Williams, & Horsfield, 1998). As opposed to locally defined gray matter structures, WM pathways connect distant regions (Catani & De Schotten, 2008; Yeh et al., 2018), cross each other, and have a complex shape including fanning, torsion, long-distance curvature, and sharp turns (Maier-Hein et al., 2017; Rheault, Poulin, Caron, St-Onge, & Descoteaux, 2020). Historically, anatomical definitions of WM pathways were scarce and came in a variety of languages, which led to coexisting definitions of the same, or similar, underlying structures. Disagreements in nomenclature (Mandonnet, Sarubbo, & Petit, 2018; Panesar & Fernandez-Miranda, 2019), evolving knowledge of projection (Chenot et al., 2019; Nathan & Smith, 1955), association (Catani et al., 2007; Geschwind, 1970), or commissural (Benedictis et al., 2016; Witelson, 1985) pathways and debate over the existence (or lack thereof) of specific connections (Forkel et al., 2014; Meola, Comert, Yeh, Stefanescu, & Fernandez-Miranda, 2015; Türe, Yaşargil, & Pait, 1997) all have contributed to variations in anatomical definitions which have led to discrepancies in the WM pathways bearing the same name (Schilling et al., 2020; Vavassori, Sarubbo, & Petit, 2021).

The complex shape and inherent representation of tractography (streamlines) make the interpretation of anatomical definitions and the subsequent dissection of WM pathway, also named virtual dissection (Catani, Howard, Pajevic, & Jones, 2002; Mori & van Zijl, 2002), challenging. Additionally, the level of familiarity with software or with data and slight differences in decision-making can all influence the dissection protocols carried out by a specific individual (intrarater reproducibility). The way the virtual dissection is performed will inherently vary across individuals performing it (interrater reproducibility). Moreover, the widespread use of tractography in population studies (e.g., aging or development) and surgery planning (e.g., deep-brain stimulation or electrode placement for epilepsy) and the diversity of anatomical definitions made it difficult to interpret results and outcomes across publications (e.g., meta-analyses). However, the need for standardization of clinical protocols is not unique to tractography (Boccardi et al., 2011; Frisoni et al., 2015) or even to neuroimaging (Sefcikova, Sporrer, Ekert, Kirkman, & Samandouras, 2020).

There are three key challenges to investigating virtual dissection reproducibility. First, clear and concise anatomical definition and dissection protocol are rarely agreed upon. Second, the time-consuming nature of manual dissection makes data gathering burdensome. Third, the digital representation of WM pathways from tractography (streamlines) makes the quantification and interpretation of reproducibility difficult and creates computational challenges.

Our main goal is to assess the consistency of raters performing repeated virtual dissection tasks and to investigate variables that impact the results. The contributions of this study are threefold. First, we quantify *intrarater* and *interrater* reproducibility for raters performing the same dissection protocol on matched data. Second, we investigate the *longitudinal* relationship between reproducibility scores

and protocol repetitions (i.e., practice). Third, we included an *online educational session* that encompasses an introduction to the project, software tutorials, and a live protocol demonstration to examine its impact against previous work that included written instruction only (pdf document).

2 | METHODS

2.1 | Study design

To perform the tasks required by the protocol, we formed a consortium of 20 collaborators (raters) from institutions in Canada, Italy, and the United States. Most collaborators are researchers familiar with tractography and the concept of virtual dissection but without any neuroanatomy background. A minority of collaborators had an advanced background in neuroanatomy. In the context of this work, collaborators' background was not part of the investigation. First, the purpose of this study is to conduct an evaluation of protocol quality after an online course. Second, as shown in the initial Tractostorm project, this distinction (presented as “nonexperts” and “experts”) had a limited impact on reproducibility scores. All collaborators in our study will be referred to as “raters” as they are manually annotating data sets. This study has been reviewed by the Internal Review Board of Vanderbilt University (#211156).

Raters attended a 2-hr online educational session on the virtual dissection software (MI-Brain; Rheault, Houde, Goyette, Morency, & Descoteaux, 2016) and followed instructions to perform the dissection protocol. The raters also had access to a detailed document on the dissection protocol (available at doi.org/10.5281/zenodo.5190145 and in Supplementary Materials). This document contains all the instructions related to the virtual dissection tasks and how to identify/locate landmarks. As the results of this work are directly related to the protocol used, reporting the exact instructions provided to the raters is crucial. This document was based on the original one from Rheault, De Benedictis, et al. (2020). Two new bundles of interest were added following the same *template* as the original document. To respect the experimental design, the raters were instructed to strictly follow the instructions, to perform the tasks on their own time in the 2 months following the online session, on the provided data, to follow the same data set ordering, and to use the same software.

Raters performed virtual dissection of the body of the CC, left AF, and left PYT on 20 data sets. Unknown to our raters, the 20 data sets were in fact five Human Connectome Project (HCP; Glasser et al., 2013) subjects that were duplicated four times (subject 1-2-3-4-5, 1-2-3-4-5, ...). In this work, the four duplicates will be referred to as “timepoints” due to the fact that our study design requires raters to perform a sequential annotation of data sets. The duplicated data sets were not scan-rescan, they were identical copies of tractograms and maps already processed by the authors. By providing identical tractograms, only the variability induced by the manual segmentations was targeted rather than variability induced by the processing pipelines. The project involved no processing from the

collaborators and aimed to quantify only how consistent the segmentation obtained from a specific protocol was. The raters were instructed to save the regions of interest (ROIs) defined by the segmentation as well as the resulting bundles. For this work, the relevant data submitted by each rater was composed of 3 (bundles) \times 5 (HCP) \times 4 (timepoints) = 60 files (trk file format).

The original data provided to the raters was the same as described in Rheault, De Benedictis, et al. (2020). Briefly, probabilistic particle filtering tractography (Girard, Whittingstall, Deriche, & Descoteaux, 2014) from constrained spherical deconvolution (Tournier et al., 2008) produced around 1.5 M streamlines for each data set. The decision to provide the same data was made to facilitate potential comparisons between both projects. Data quality and processing were adapted for the current study design. Since the data had already been used in a similar study, uncertainty related to computer performance during the virtual dissection was low.

2.2 | Dissection protocol

Our goal is to evaluate the capacity of raters to perform repeated virtual dissection tasks. These tasks are limited to ROIs “drawing” (i.e., shape, size, and position) on provided data. The raters only had to open the software and load the preprocessed data (tractograms and maps), then follow instructions to identify anatomical landmarks as described.

One of the limiting factors in the initial Tractostorm project was the use of only one bundle of interest. This was due to the initial complexity of the study design and the number of unknown variables. Using the same template and aiming for the same level of clarity, a dissection protocol was defined for each of the three bundles of interest (CC, AF, and PYT). The prior work helped with refining the project and allowed us to expand the number of bundles. The decision to limit dissection to one hemisphere (left AF and left PYT) was made to reduce the workload for our raters.

As part of the protocol, 15 ROIs had to be drawn per data set. Then, three bundles had to be dissected using a subset of ROIs and rules such as inclusion and exclusion. Once a data set was dissected and the required files saved, modifications were not allowed. If a major mistake (e.g., mixing up left/right) was observed before the following data set was started, corrections were allowed.

To ensure a similar level of familiarity with the software used for the project among all raters, the software and protocol were introduced in a 2-hr online educational session. The recording of the online educational session and a document describing in detail the protocol were made available to the raters. Collaboration between raters was not allowed. Minimal interaction with the principal investigator was allowed to confirm tasks' interpretation (software installation, data set ordering, files to save, how to submit, etc.). Following the course, the principal investigator stayed available for questions as well as encouraged to practice the protocol and experience the software if needed. However, due to time zone differences, some raters (in Europe)

reached the end of their workday. Raters were allowed to ask general questions (that were emailed to everyone via email if necessary).

Raters had to complete the tasks on their own schedule within 2 months following the online course. This was considered a realistic timeline that would accommodate all collaborators considering the various stages of their academic career/schedule during the COVID-19 pandemic and the fact that the expected duration of the task was estimated to be 10–20 hr. This personal freedom in the submission timeline was also allowed in the first Tractostorm project and justified because of the difficulty to supervise/control the schedule of 20 international researchers.

2.3 | Analysis

To quantify the reproducibility between timepoints (intrarater) or across the group (interrater) within a single timepoint (Figure 1), metrics adapted to the data representation were chosen. To accurately portray agreement and for consistency with the prior work of Rheault, De Benedictis, et al. (2020), three metrics were chosen for the analysis.

2.3.1 | Dice score of voxels

Quantify spatial agreement of the overall volume occupied by a dissection. From the bundle, any voxels traversed by at least one streamline are set to 1, resulting in a binarized volume of the bundle (mask). This is then compared to the binarized volume of another data set. The number of streamlines *does not* influence the results outside the volume they occupy. This metric is highly sensitive to outliers because outliers quickly increase the nonoverlapping volume.

2.3.2 | Dice score of streamlines

Quantify the agreement of the exact selection of streamlines. Since compared data sets were matched across raters, streamlines can be compared directly. The value for this metric lies between 0 and 1 and represents the ratio of streamlines that are *identical* in both data sets to the total number of streamlines in both data sets. A perfect score is much harder to achieve since this metric is inherently linked to streamline count while Dice score of voxels is not.

2.3.3 | Correlation of density maps

Measure the coherence between density maps. A large overlap between bundles' cores is more important than the sparse overlap of rare spurious streamline and/or outlier. The goal of this metric is to assess whether the distribution of streamlines in space is similar. This allows bundles with different streamline counts to reach high scores *if* their density maps are correlated.

FIGURE 1 Representation of the study design. Twenty collaborators (raters) contributed by carrying out our protocol, each had three bundle dissections to perform for each of the 20 data sets. The 20 data sets were five HCP subjects (missing from the figure) each with four timepoints. The total submitted data consisted of 1,200 bundles and 6,000 ROIs. HCP, Human Connectome Project

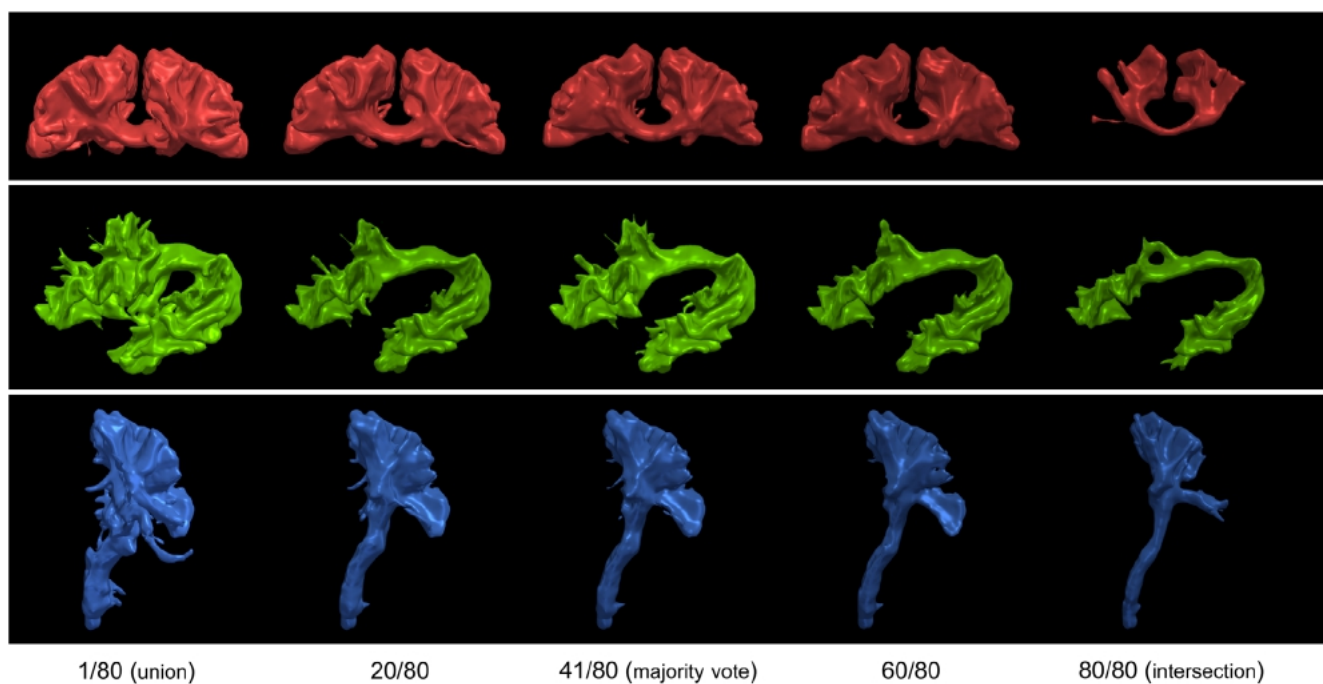
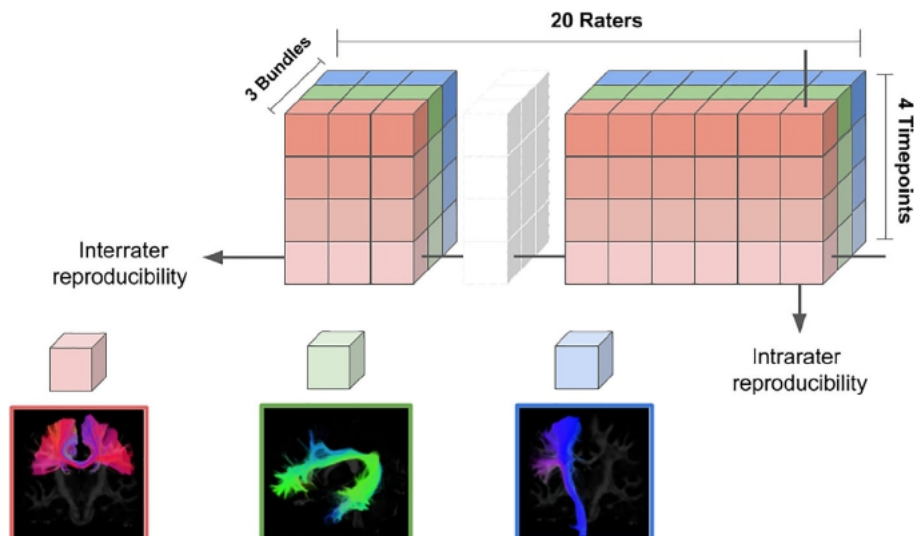


FIGURE 2 Example of gold-standard generation obtained by using a voting approach. Each row shows the bundles of interest and represents a smooth isosurface at the selected threshold. From left to right, multiple voting ratios from 0.0125 (union) to 0.5125 (majority vote) to 1.0 (intersection) from 80 segmentations of the first subject. At each increase in the voting threshold, the number of voxels decreases. A minimal vote set at 1 out of 80 (1/80 or 0.0125; left) is equivalent to a union of all segmentations while a vote set at 80 out of 80 (right) is equivalent to an intersection between all segmentations. Both of these thresholds are prone to variations due to outliers in the submitted data. Thresholds at 25, 50, and 75% generate similar group averages due to the raters' high spatial consistency, a majority-vote approach was selected for its intuitiveness and coherence with the first Tractostorm project

Since no single rater can be said to have the *right* dissection, we rely on a group average (majority vote) to establish our gold standard. In the first Tractostorm project, only the experts' group was used to generate the gold standard and establish that nonexperts were closely similar to the gold standard (both groups delineated bundles that were very similar on average). These results demonstrated that expertise in neuroanatomy is not required to follow our segmentation protocol and achieve a gold standard that is anatomically meaningful (see Figure 2).

Similar to Rheault, De Benedictis, et al. (2020), metrics that include true negatives in their computation were excluded as they tend to converge toward a perfect score because true positives are overrepresented by an order of magnitude or two. A typical volume (or tractogram) contains millions of voxels (or millions of streamlines), and the typical dissection contains only thousands of voxels (or thousands of streamlines). The chosen binary classification metrics are kappa, precision, and sensitivity for both the voxels and the streamline representations.

Statistical differences between HCP subjects or between bundles were tested using a Mann–Whitney rank test with a significance threshold of 0.01. Longitudinal trends were tested using a linear mixed model, using bundles as different groups and accounting for random effects from raters, where the null hypothesis is that the slope is zero (significance threshold of 0.01).

3 | RESULTS

3.1 | Qualitative

During the data-gathering phase of the project, despite the protocol requiring a strict filename convention, various naming errors demonstrated that following instructions, even simple ones, is prone to errors. However, these kinds of errors were easy, but time-consuming, to correct manually.

Upon reception of the data, each bundle was visually inspected (and naming convention verified). From prior experience, the PYTs seem to have been more consistently segmented than in the previous study (shown in the last row of Figure 3). Extreme variations were less common, and major outliers were rarer in the PYT than in the initial Tractostorm project.

The vast majority of submissions were close to what was expected from anatomical knowledge. The general shape and position

matched with the known anatomy the protocol attempted to dissect. As seen in Figure 3, no major misinterpretation or obviously mistaken dissection was found. Despite the noisy nature of probabilistic tractography and the admittedly difficult task of interpreting and executing the tasks, the submitted data appeared consistent and rarely contained spurious streamlines.

3.2 | Quantitative

3.2.1 | Scalar measurements

When performing the tasks on the exact same data, consistent measures are expected, but as shown in Figure 4, the resulting dissections cover a wide range of scalar measures. While some measures are consistent, that is, average fractional anisotropy (FA) or average length, others are much more variable, that is, streamline count and volume. Scalar measurements are *disconnected* from the spatial agreement, which is why one measure can be extremely stable (e.g., average FA) and another extremely variable (e.g., volume). Since some of the reported measures do not follow a Gaussian distribution, values are reported as (median \pm interquartile range) for simplicity. The average FA is stable across bundles (0.45 ± 0.01), despite having a commissural, an association, and a projection pathway with variable volume (ranging from 40,000 mm³ to more than 125,000 mm³). This simply

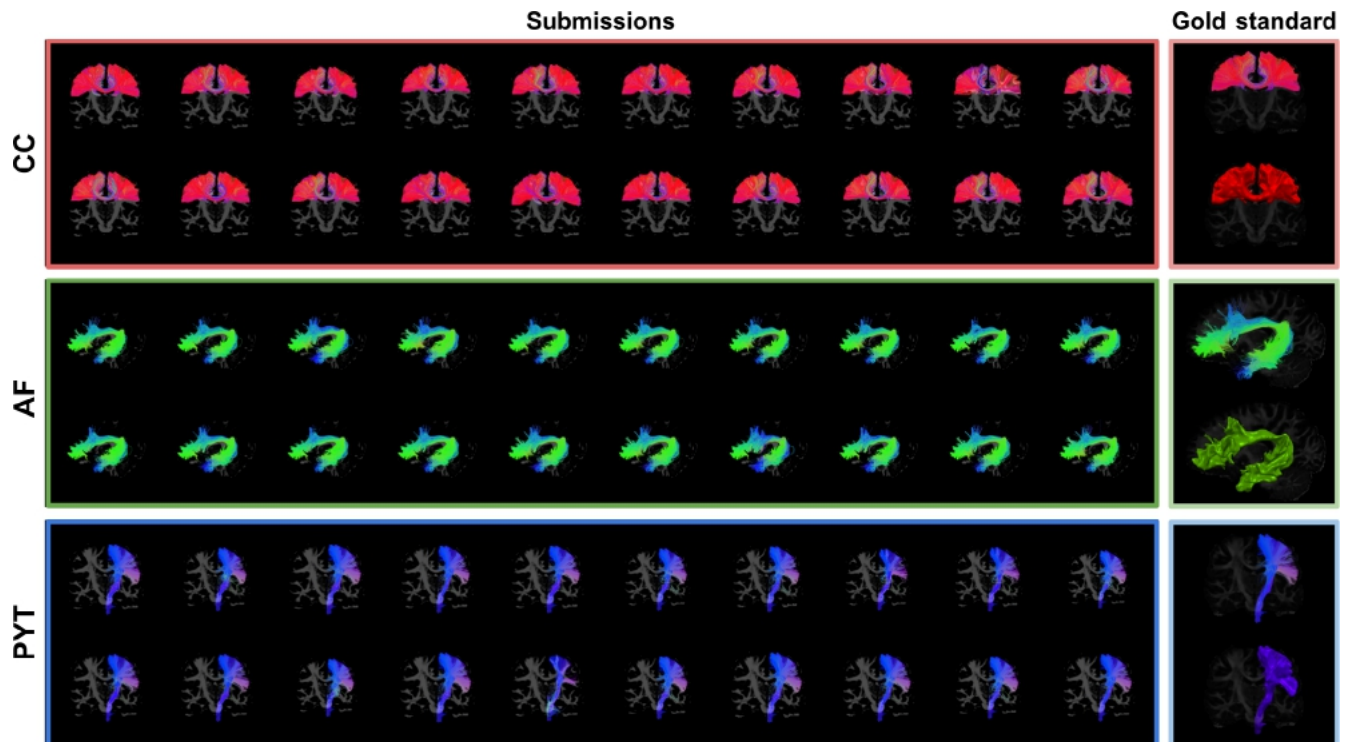


FIGURE 3 Mosaic of dissections of the first timepoint of the first HCP subject from 20 raters (left), all dissections look extremely similar. On the right, the average dissection (gold standard) in both the streamlines and the voxel representations. The coloring is based on the orientation of each streamline, where the X/Y/Z differences are mapped to R/G/B. To be considered part of the gold standard, elements had to be labeled in at least 50% of dissection associated with each subject. The PYT had a more consistent spatial coverage compared to the first Tractostorm project (only bundle in common). AF, Arcuate fasciculus; CC, corpus callosum; HCP, Human Connectome Project; PYT, pyramidal tract

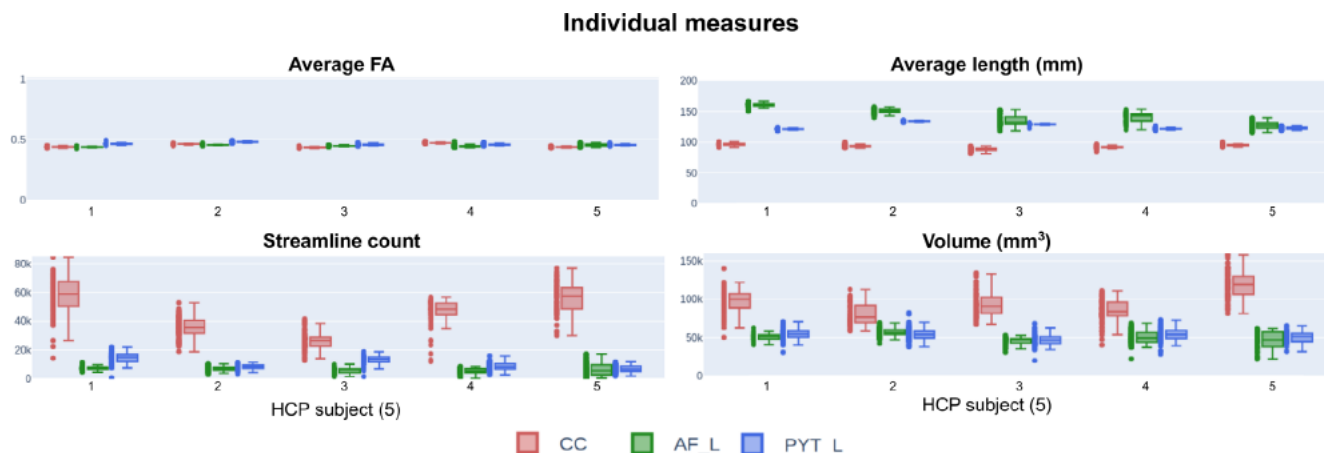


FIGURE 4 Individual measures for each HCP subject (1–5). Each dot represents one submitted bundle, and each box plot represents 80 files (20 raters \times 4 timepoints = 80). This shows the impacts of dissection variability on observed measures. These are measures that are often reported in the literature but do not directly quantify spatial agreement (different volumes can lead to the same average FA). AF, Arcuate fasciculus; CC, corpus callosum; FA, fractional anisotropy; HCP, Human Connectome Project; PYT, pyramidal tract

shows that drastically different bundles with variable size, shape, and location all lead to the same average FA (with little to no deviation).

Some relationships between bundles are observable across HCP data sets (true at most/all of 20 timepoints). For example, the average length of the AF is systematically higher (143.45 ± 13.09) than both the CC (93.24 ± 3.43) and the PYT (126.00 ± 5.25) or the volume of the CC ($94,827 \pm 20,213 \text{ mm}^3$) is higher and more variable than both the AF ($50,101 \pm 8,403 \text{ mm}^3$) and PYT ($52,282 \pm 8,232 \text{ mm}^3$).

3.2.2 | Intrarater agreement

In Figure 5, the intrarater reproducibility scores show a high level of consistency for voxel-based metrics (correlation of density maps and Dice score of voxels). The AF obtained lower scores on average for metrics that take into account streamlines (correlation of density maps and Dice score of streamlines), which indicates that the overall spatial agreement is good, but the streamlines themselves were not spatially distributed similarly.

On average, Dice scores of voxels achieve very close results for all bundles (CC 0.89 ± 0.06 , AF 0.89 ± 0.08 , and PYT 0.88 ± 0.07). However, as seen in Figure 5, these scores vary from subject to subject. This is particularly apparent for the streamline-based metrics. When each rater was analyzed individually, it can be observed that reproducibility is not equal across all raters. However, no single rater systematically scored very high/low reproducibility.

3.2.3 | Longitudinal interrater agreement

No statistically significant longitudinal difference in interrater reproducibility is observable when data are analyzed longitudinally (in the chronological order of dissection, for each HCP subject). As shown in Figure 6, no relationship between timepoints and any metrics can be distinguished.

No single rater was responsible for systematically different dissections. Submissions that are completely inconsistent with the group are rare. This leads to only a few reproducibility scores being much lower, which contributes to increasing the interquartile range. Voxel-based representation produces higher and more stable reproducibility scores.

Reproducibility scores do not vary across bundles for voxel-based metric (Dice score of voxels: CC 0.83 ± 0.08 , AF 0.84 ± 0.10 , and PYT 0.83 ± 0.07). The metrics that take streamline density into account do vary across bundles and across subjects. For example, the AF at timepoints associated with the first HCP subject achieve very high interrater scores for all metrics (e.g., a correlation of density maps of 0.97 ± 0.02). However, the timepoints associated with the last HCP subject are much lower and more variable across all metrics (e.g., a correlation of density maps of 0.64 ± 0.31). This is a similar observation to the patterns across bundles/subjects seen in the intrarater section.

3.2.4 | Binary classification

To evaluate binary classification metrics, the dissection of each rater was compared to the group average (gold standard; Figure 7). Binary classification metrics show that the group of raters generally obtained high levels of spatial agreement. The stability of all binary classification metrics across timepoints indicates an absence of a relationship between protocol learning/practice and dissection agreement on the group level. No statistically significant longitudinal difference is observable (linear mixed model).

The balance of high precision (how many selected elements are relevant) around 0.90 ± 0.07 for the voxel representation and high sensitivity (how many relevant elements are selected) around 0.89 ± 0.10 for the voxel representation indicates a very high spatial agreement at the group levels. As expected, the streamline representation

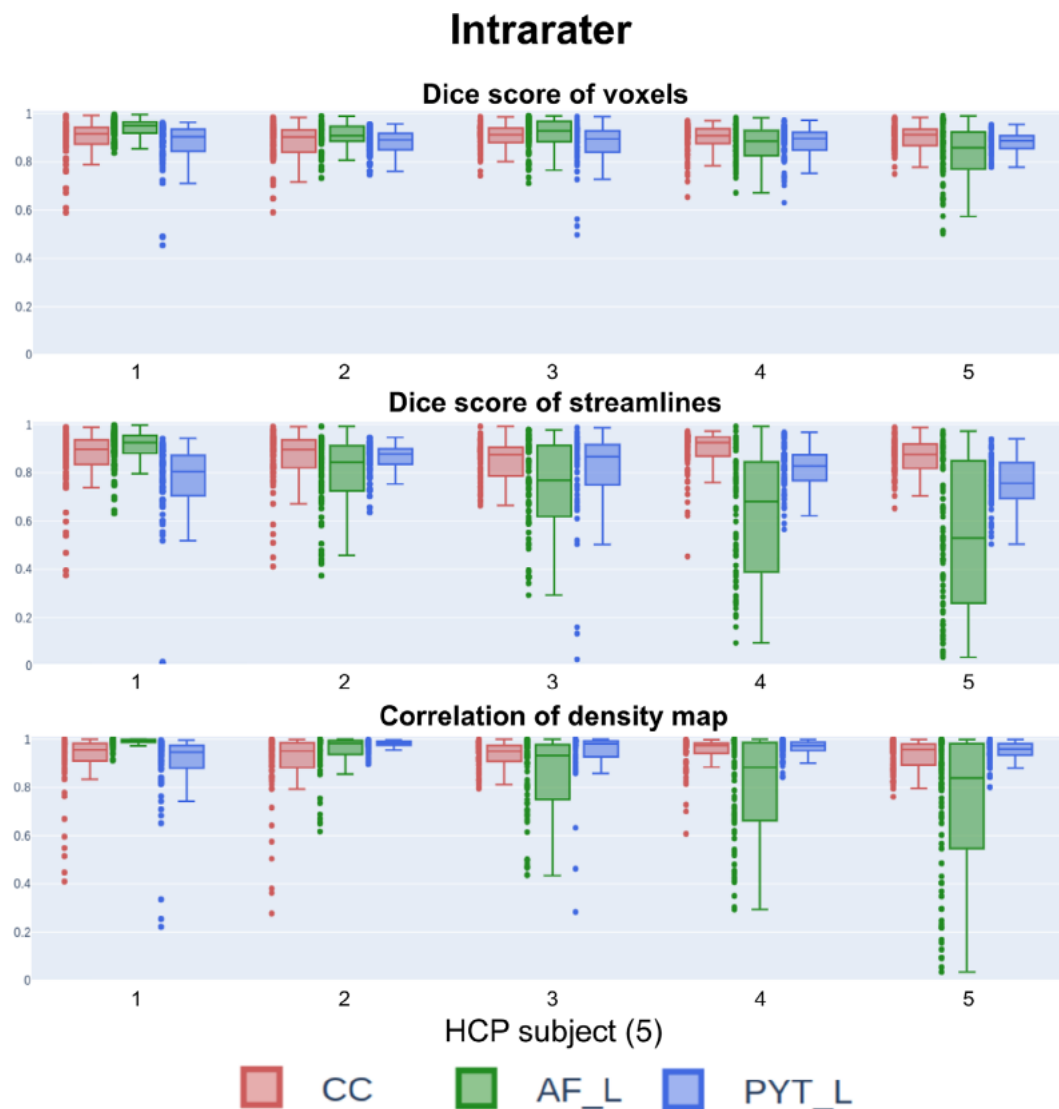


FIGURE 5 Reproducibility scores for intrarater agreements for all subjects. There is no longitudinal/temporal component to this figure, and all timepoints (per HCP subject) are needed to compute the intrarater scores. As expected, the voxel representation (Dice score) shows high reproducibility across bundles and HCP subjects. Only one bundle (AF) was highly impacted by anatomical differences (across subjects) for the streamline representation. AF, Arcuate fasciculus; CC, corpus callosum; HCP, Human Connectome Project; PYT, pyramidal tract

produces lower scores on average than the voxel representation. Despite being lower and more variable, precision of streamlines (CC: 0.89 ± 0.08 , AF: 0.72 ± 0.22 , and PYT: 0.85 ± 0.09) and sensitivity of streamlines (CC: 0.85 ± 0.14 , AF: 0.75 ± 0.27 , and PYT: 0.81 ± 0.16) are well-balanced. The pattern of lower scores for the AF associated with the first HCP subject to the last HCP subject is still observable.

4 | DISCUSSION

Each execution of the protocol by the raters is slightly different, but there is no trend over the longitudinal component of our experiment. The stability of reproducibility scores over time (for each subject, across timepoints) shows that interpretation and execution did not

change at the group level. The effect of practice had no observable importance in the process of virtual dissection. This is a reassuring result, once raters are introduced to the software and tasks at hand, their interpretation and execution (as a group) do not significantly vary (positively or negatively).

Results from the three bundles of interests show that reproducibility varies across pathways. This is in line with previous works (Boukadi et al., 2019; Cousineau et al., 2017; Wakana et al., 2007). It is unknown whether the dissection rules and landmarks are inherently harder to define or if some bundles are simply more prone to spurious streamlines and outliers (e.g., more ROIs needed to be defined, and therefore the small variations or “mistakes” add up). Future work involving a formal analysis of ROIs (saved by raters as part of this protocol) will aim to disentangle this question and to provide insight into

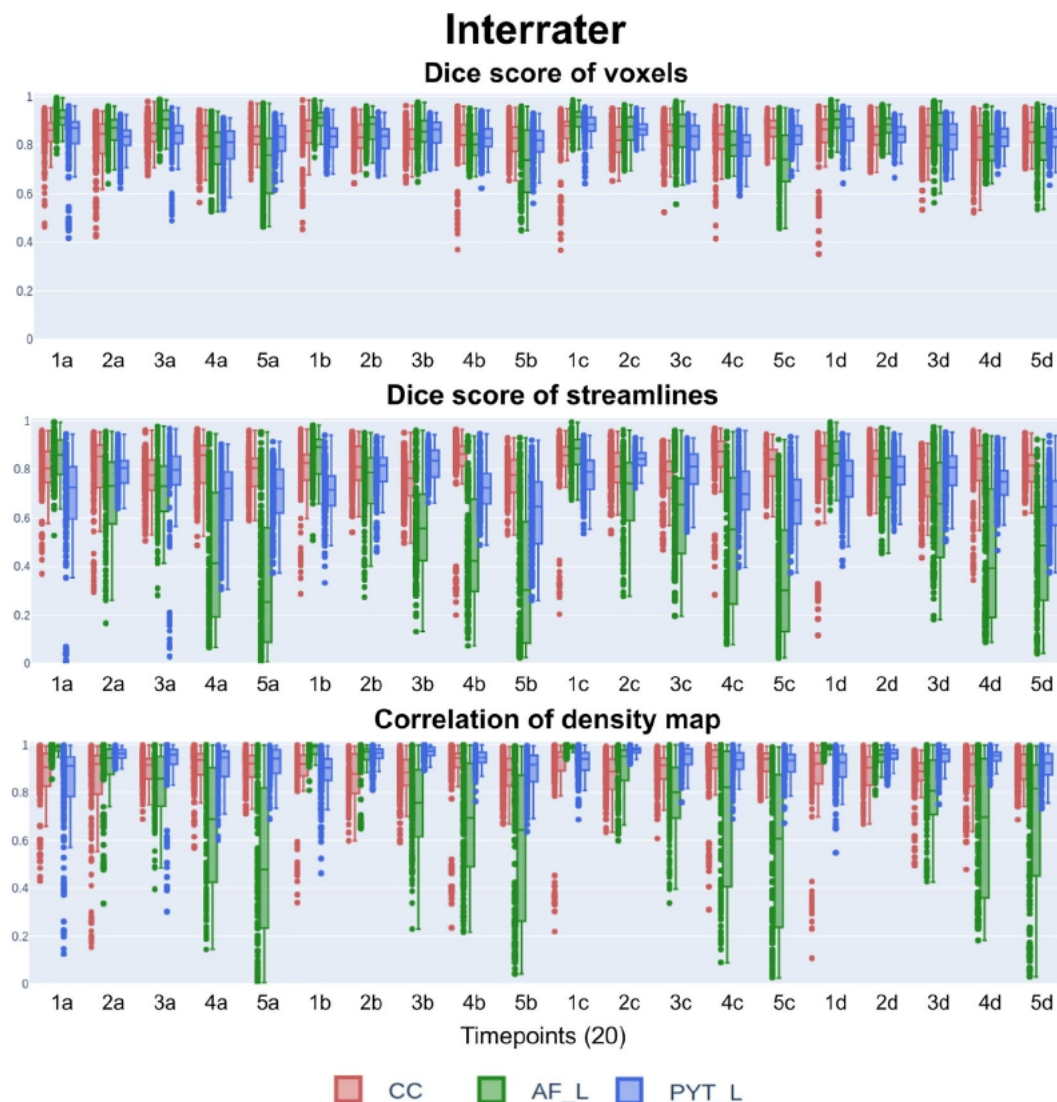


FIGURE 6 Reproducibility scores (interrater) for all timepoints showing agreement at the group level. The x-axis represents first-to-last subject (1–5) and first-to-last repetition (a–d). No discernable temporal pattern can be observed, and interrater agreement remains stable as the amount of “practice” increases. Similar to the intrarater agreement, the AF reproducibility scores (streamline representation) seem to be more difficult to segment consistently at the group level depending on the HCP subject. AF, Arcuate fasciculus; CC, corpus callosum; HCP, Human Connectome Project; PYT, pyramidal tract

good practice for future protocols development and/or inform anatomical definition at large. We believe such an investigation deserves its own line of analysis.

An interesting pattern is observable for the AF: The best and worst intrarater and interrater reproducibility scores were obtained in the first and the last HCP subject, respectively. Preliminary investigation shows more variability with some ROIs associated with the AF may be the cause. This indicates that anatomical differences can have an impact on the identification of landmarks and drastically influence the reproducibility/quality of dissection. Identifying the exact source of this unintuitive variability is crucial to improving the current protocol. It could be due to an ROI being misplaced and thousands of streamlines that generally overlap with the whole bundle to be discarded. This would affect the density map and the correlation metrics without a major impact on the overall volume of the bundle.

Raters' reproducibility scores were well distributed, but some outperformed others. Furthermore, some raters had closer similarities to the group average (which is considered anatomically meaningful). This could indicate there is such a thing as “good rater” and “bad rater”. Not only is a good rater expected to have a high intrarater reproducibility score, but they are expected to have a high agreement with the group average. This is referred to as *master tracers/raters* in European Alzheimer's Disease Consortium - Alzheimer's Disease Neuroimaging Initiative hippocampus project (Frisoni et al., 2015).

4.1 | Generalization of protocols reproducibility

The results from multiple bundles, as well as a modified teaching approach, confirmed the hypothesis from the first Tractostorm study

Binary classification

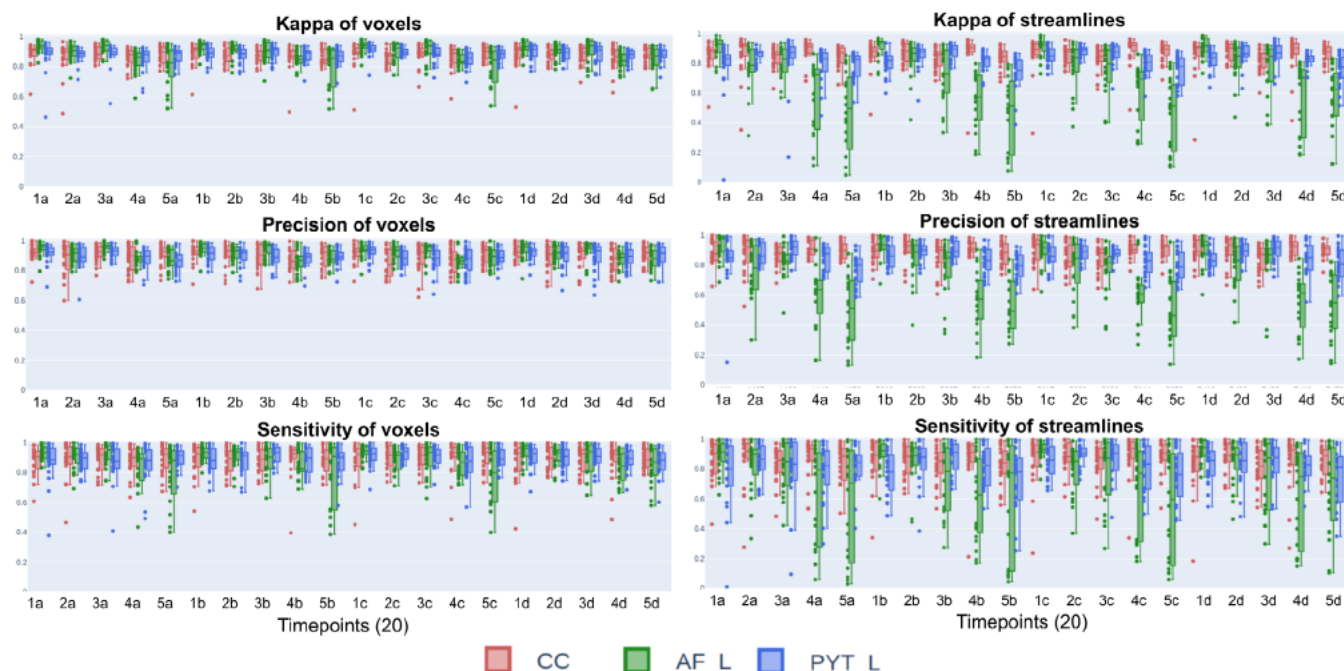


FIGURE 7 Reproducibility scores (gold standard) for all timepoints showing agreement with the group average. This shows that despite variation at the group level, on average, everyone segmented approximately the same bundle. This means that two raters can get variations of the same bundle and possibly be close to each other, but on average, a few raters performing the same task will always converge toward an average dissection. AF, Arcuate fasciculus; CC, corpus callosum; PYT, pyramidal tract

that reproducibility scores cannot be easily generalized. Each protocol modification has the potential to drastically affect reproducibility. As hypothesized in Rheault, De Benedictis, et al. (2020), we confirmed that different bundles have different reproducibility scores. This confirms that any modification (e.g., teaching method, software) or addition (e.g., new ROIs, new bundles) to the protocol will likely change the reproducibility scores and thus generalization is *likely* impossible.

The major differences of streamline representation metrics (e.g., Dice score of streamlines) between HCP subjects for the AF indicate that some anatomical structures are harder to define/find and can have a bundle-specific impact on reproducibility. This could be amplified when dealing with data sets with a wide range of ages or pathology. This further supports that generalization is extremely difficult and reproducibility should be studied independently for each bundle.

Modifications to protocols should trigger a reproducibility evaluation, and it should be targeted for a *somewhat* specific range of audiences, data sets, and populations. For example, this work was mainly designed for raters without neuroanatomy background on young/healthy subjects from the HCP database. However, a silver lining is that some *flexibility* is possible when targeting the scope of a protocol. Rheault, De Benedictis, et al. (2020) demonstrated that the experts and nonexperts group distinction (with and without formal anatomy background) had a minimal effect for spatial agreement in voxel representation (Dice score of voxels). Furthermore, TractEM (Bayrak et al., 2019) showed that acquisition quality (angular/spatial

resolution) did not have a major influence on the agreement (both Dice score of voxels and correlation of density map). Finally, this work showed that by leveling the familiarity with the software and the protocol with an online educational session, virtual dissection tasks can reach a very high spatial agreement for every rater and remain stable. This is reassuring for those aiming for standardized WM pathway dissection protocols or for automatic dissection methods that rely on curated bundles obtained from such protocols.

4.2 | Future projects aiming to define WM pathways

Widely different protocols are preventing the comparison across publications in the literature and limit the potential for meta-analysis. Standardized anatomical definitions are clearly needed. Both theoretical (with no regard for acquisition, local modeling and tractography reconstruction), and practical definitions are needed. The data generated by this work will be made available online (<https://doi.org/10.5281/zenodo.5190145>) in March 2022.

Theoretical definitions must refer to conceptual landmarks and regions and convey the general shape, orientation, and terminations. They must aim to be distinct enough between bundles while encompassing a variety of practical definitions. Such definitions should refer to anatomical structures of the brain and not be tied to specific contrasts or processing. Work such as Catani & De

Schotten, 2008 and Mandonnet et al., 2018 can be considered in this category. These WM atlases explain the reasoning behind the subdivisions (function, topology, connectivity, etc.) and have a broad presentation of WM pathways' location, shape, and regions they are expected to connect.

Practical definitions must refer to a specific execution of a theoretical definition. They can change according to the target audience (e.g., experts vs. nonexperts), time requirements (e.g., quick approximation vs. careful delineation), visualization software (e.g., MI-Brain vs. TrackVis), or underlying processing (e.g., diffusion tensor imaging vs. high angular resolution diffusion imaging, deterministic vs. probabilistic). This also applies to automatic dissection methods. Work such as David et al. (2019) or Catani et al. (2013) describes a single WM pathway and their cortical terminations, shape, and surrounding anatomical landmarks. These descriptions are not explicit enough for replicable results, and some of the steps are inherently linked to processing choices. However, they can be considered an attempt at a practical definition even if details are missing. For

instance, TractEM (Bayrak et al., 2019) provides detailed guidelines for whole-brain tractogram dissections into bundles with processing/software instructions; this qualifies as a practical definition.

Even slight modifications to manual (e.g., number of ROIs, software update, description of landmarks) or automatic methods (e.g., loss functions, atlases, clustering methods) can have unforeseen impacts on reproducibility (bundle-specific influences, algorithms that break down due to support variations in processing, etc.). This is why standardization is important, and such a resource-intensive investigation (e.g., the current work) repeated frequently for minor variations would be a waste.

A subsequent project is already planned, and it aims to investigate the ROIs submitted by our raters to inform future practical definitions. The variability of ROIs across raters and the influence of shape and distance will provide insight into future protocol iterations. The general aim is to help to design future protocols that can vary in robustness, time restrictions, or complexity.

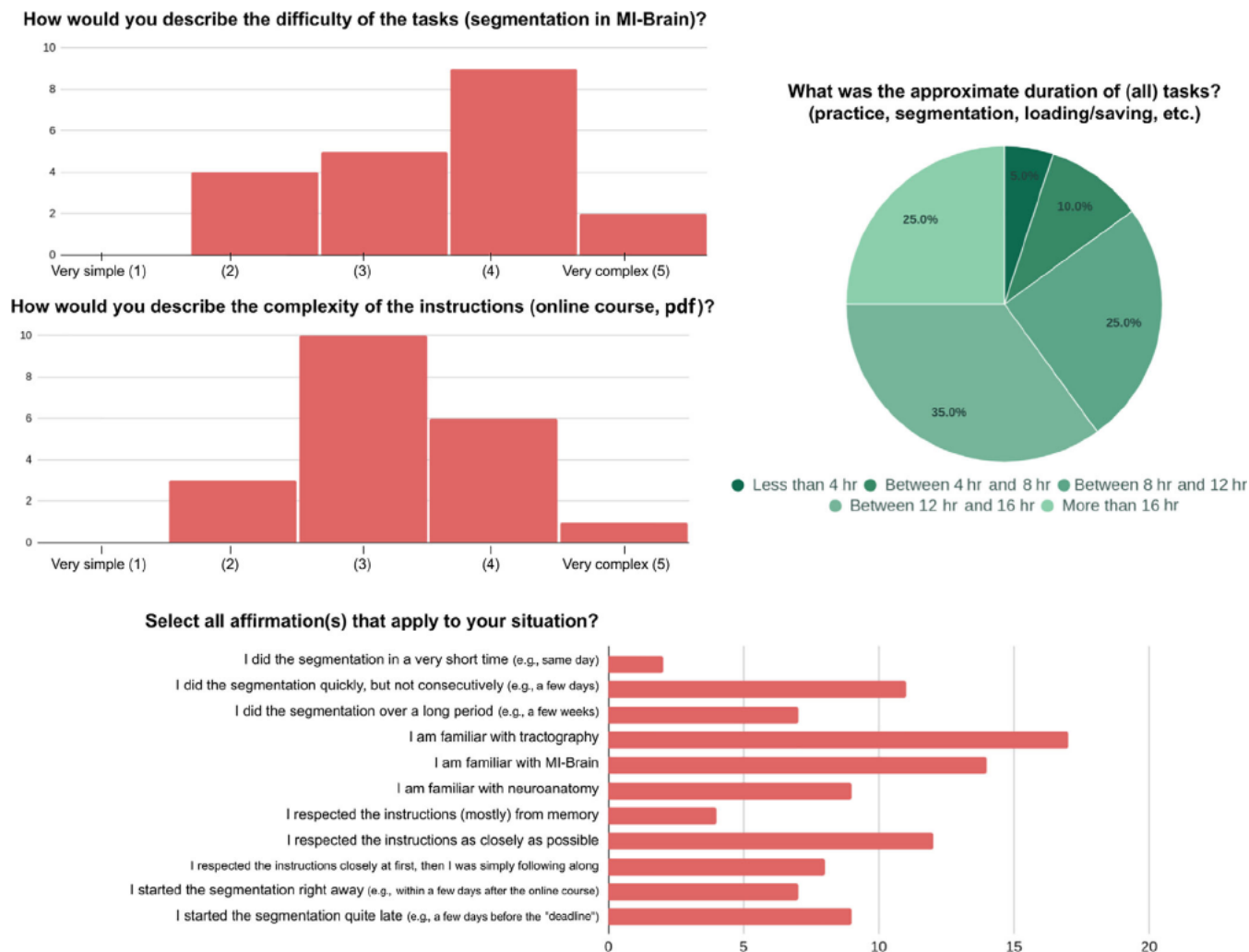


FIGURE 8 Results from the survey that portray a general picture of our group of raters and how they experienced/conducted the tasks. The affirmations (bottom) are not quantitative and rely on a personal assessment only (e.g., “I am familiar”, “I respected”). Twenty collaborators responded to the survey

4.3 | The impact of the online educational session

Observations and data from both iterations of the Tractostorm studies show the importance of accounting for external variables (experience with the software, anatomical knowledge, and familiarity with the task to be performed). The current project indicates that even one, relatively short, online educational session can have a major impact on the quality of results of a multi-institutions collaboration on virtual dissection. In our current work, the online educational session encompassed an introduction to the project, a software tutorial, a demonstration of the protocol, and question and answer session.

Including a 2-hr online educational session with a simple written document increased the average Dice score of voxels (for the PYT) from 0.65 to 0.85 with an interquartile range decreased from 0.15 to 0.08. It is unknown if this is due to better identification of landmarks or general familiarity with the tasks and/or the software. We cannot identify the exact component of the online educational session that helped the most, and only that the online educational session as a whole contributed to the improved reproducibility.

This could change/inform how we teach tractography and virtual dissection for clinical purposes as well as in research. This work also could provide insight into ways to convey information about shapes and landmarks of WM pathways when described in anatomy textbooks, for example. For an anatomical definition to be useful, it has to be anatomically valid and easy enough to communicate to others so most interpretations are anatomically valid as well.

4.3.1 | Postexperiment survey of raters

A survey conducted with our collaborators helped us to understand how they perceived the experience and to give us insight into how the experiments were conducted. While the answers provide only personal opinions, they are a source of information on the perceived workload, difficulty, and general impression of the project.

Overall, the project was appreciated by our collaborators despite its heavy workload. During the planning phase, it was estimated (to plan workload) that each bundle dissection would take 5–10 min (15–30 min per data set, 5–10 hr in total). As seen in Figure 8, these values were underestimated, and from the feedback we received, this is likely because the first subject or two took much longer and the 15 min per data set was achieved only toward the end for most raters. Instructions' complexity was seen as "simple" while the software complexity was perceived as greater than the instructions. This reinforces the intuition that software could be a major source of variability.

The timeline of execution could also be an important variable to investigate. After the course and on their own time, raters were allowed to decide when to execute the tasks and how many data sets to do each time. This freedom was also allowed in the first Tractostorm project and mainly due to the difficulty to supervise or control the schedule of 20 researchers spread across North America and Europe. The allowed window for raters to submit their segmentation data was open for 2 months after the online course. The vast

majority of raters submitted their delineation between Week 4 and Week 8 with two exceptions. One rater finished the tasks within 1 week of the online course, and another finished the tasks 2 weeks after the allowed window (authorized by the principal investigator due to personal circumstances).

5 | CONCLUSION

In this work, we quantified the effect of practicing and learning a protocol for WM pathway dissection. Using matched data and a large group of raters, we quantified their individual agreement (intrarater) as well as their group agreement (interrater). We demonstrated that as raters practice, their interpretation and execution remain stable. Despite the global nature of WM pathways, high *spatial/voxel* reproducibility can be achieved. However, we observe that modifying the teaching method has a large effect. The online educational session on the software and protocol had a major positive impact (30% higher median and 50% lower interquartile range) on the reproducibility of the PYTs (only bundle in common across both studies).

It is important to note that variations between both Tractostorm projects indicate that bundle dissection, even if designed with a similar template and the same level of detail, cannot be easily generalized, and so, careful evaluation must be systematically performed. This evaluation of the impact of a teaching method on the protocol results is an essential step to improve the future design of WM dissection protocols.

ACKNOWLEDGMENT

This work was supported by the National Institutes of Health (NIH) under award numbers R01EB017230, P50HD103537, and T32EB001628, and in part by ViSE/VICTR VR3029 and the National Center for Research Resources, Grant UL1 RR024975-01.

Each collaborator's contribution to the project was made possible by various sources of funding:

- Leon Cai was supported by NIH/NIGMS, grant number 5T32GM007347.
- Viljami Sairanen was supported the Orion Research Foundation sr, the Instrumentarium Science Foundation sr., and the Emil Aaltonen Foundation.
- Pietro Bontempi was supported by Verona Brain Research Foundation (high-field MRI for the study of peripheral nerve microstructure).
- Guido Guberman was supported by the Vanier Canada Graduate Scholarship.
- Maggie Roy was supported by The Mathematics of Information Technology and Complex Systems (MITACS).
- Charles Poirier, Gabrielle Grenier, and Philippe Karan were supported by the scholarship from Natural Sciences and Engineering Research Council (NSERC) and Fonds de Recherche du Québec Nature and Technologies (FRQNT).
- We thank the Université de Sherbrooke institutional research chair in Neuroinformatics that supports Maxime Descoteaux and his team.

- Sami Obaid was supported by the Savoy Foundation studentship and from scholarships from the Fonds de Recherche du Québec - Santé (277581).

DATA AVAILABILITY STATEMENT

The data provided to the raters are openly available on Zenodo at <https://zenodo.org/record/5190145#.YY7qRnVKhH5> in 2022. The provided data are from the Human Connectome Project (HCP) The data that support our results (tracers annotations) will be available at the same link in 2022.

ORCID

Francois Rheault  <https://orcid.org/0000-0002-0097-8004>
 Guido I. Guberman  <https://orcid.org/0000-0002-4422-2225>
 Sami Obaid  <https://orcid.org/0000-0002-8650-2444>
 Simona Schiavi  <https://orcid.org/0000-0003-1641-186X>
 Laurie E. Cutting  <https://orcid.org/0000-0002-2362-6028>
 Laurent Petit  <https://orcid.org/0000-0003-2499-5367>

REFERENCES

- Bayrak, R.G., Schilling, K.G., Greer, J.M., Hansen, C.B., Greer, C.M., Blaber, J.A., ... Landman, B.A. (2019). TractEM: Fast protocols for whole brain deterministic tractography-based white matter atlas. *bioRxiv*, 651935.
- Benedictis, A., Petit, L., Descoteaux, M., Marras, C. E., Barbareschi, M., Corsini, F., ... Sarubbo, S. (2016). New insights in the homotopic and heterotopic connectivity of the frontal portion of the human corpus callosum revealed by microdissection and diffusion tractography. *Human Brain Mapping*, 37, 4718–4735.
- Boccardi, M., Ganzola, R., Bocchetta, M., Pievani, M., Redolfi, A., Bartzokis, G., ... Frisoni, G. B. (2011). Survey of protocols for the manual segmentation of the hippocampus: Preparatory steps towards a joint EADC-ADNI harmonized protocol. *Journal of Alzheimer's Disease*, 26, 61–75.
- Boukadi, M., Marcotte, K., Bedetti, C., Houde, J.-C., Desautels, A., Deslauriers-Gauthier, S., ... Brambati, S. M. (2019). Test-retest reliability of diffusion measures extracted along white matter language fiber bundles using HARDI-based tractography. *Frontiers in Neuroscience*, 12, 1055.
- Catani, M., Allin, M. P., Husain, M., Pugliese, L., Mesulam, M. M., Murray, R. M., & Jones, D. K. (2007). Symmetries in human brain language pathways correlate with verbal recall. *Proceedings of the National Academy of Sciences*, 104, 17163–17168.
- Catani, M., & De Schotten, M. T. (2008). A diffusion tensor imaging tractography atlas for virtual in vivo dissections. *Cortex*, 44, 1105–1132.
- Catani, M., Howard, R. J., Pajevic, S., & Jones, D. K. (2002). Virtual in vivo interactive dissection of white matter fasciculi in the human brain. *NeuroImage*, 17, 77–94.
- Catani, M., Mesulam, M. M., Jakobsen, E., Malik, F., Martersteck, A., Wieneke, C., ... Rogalski, E. (2013). A novel frontal pathway underlies verbal fluency in primary progressive aphasia. *Brain*, 136, 2619–2628.
- Chenot, Q., Tzourio-Mazoyer, N., Rheault, F., Descoteaux, M., Crivello, F., Zago, L., ... Petit, L. (2019). A population-based atlas of the human pyramidal tract in 410 healthy participants. *Brain Structure and Function*, 224, 599–612.
- Cousineau, M., Jodoin, P.-M., Garyfallidis, E., Côté, M.-A., Morency, F. C., Rozanski, V., ... Descoteaux, M. (2017). A test-retest study on Parkinson's PPMI dataset yields statistically significant white matter fascicles. *NeuroImage: Clinical*, 16, 222–233.
- David, S., Heemskerk, A. M., Corrivetti, F., Thiebaut De Schotten, M., Sarubbo, S., Corsini, F., ... Leemans, A. (2019). The superoanterior fasciculus (SAF): A novel white matter pathway in the human brain? *Frontiers in Neuroanatomy*, 13, 24.
- Fennema-Notestine, C., Hagler, D. J., Jr., McEvoy, L. K., Fleisher, A. S., Wu, E. H., Karow, D. S., & Dale, A. M. (2009). Structural MRI biomarkers for preclinical and mild Alzheimer's disease. *Human Brain Mapping*, 30, 3238–3253.
- Forkel, S. J., de Schotten, M. T., Kawadler, J. M., Dell'Acqua, F., Danek, A., & Catani, M. (2014). The anatomy of fronto-occipital connections from early blunt dissections to contemporary tractography. *Cortex*, 56, 73–84.
- Frisoni, G. B., Jack, C. R., Jr., Bocchetta, M., Bauer, C., Frederiksen, K. S., Liu, Y., ... EADC-ADNI Working Group. (2015). The EADC-ADNI harmonized protocol for manual hippocampal segmentation on magnetic resonance: Evidence of validity. *Alzheimer's & Dementia*, 11, 111–125.
- Gasparini, C., Rovaris, M., Sormani, M., Bastianello, S., Pozzilli, C., Comi, G., & Filippi, M. (2001). Intra-observer, inter-observer and inter-scanner variations in brain MRI volume measurements in multiple sclerosis. *Multiple Sclerosis Journal*, 7, 27–31.
- Geschwind, N. (1970). The organization of language and the brain. *Science*, 170, 940–944.
- Girard, G., Whittingstall, K., Deriche, R., & Descoteaux, M. (2014). Towards quantitative connectivity analysis: Reducing tractography biases. *NeuroImage*, 98, 266–278.
- Glasser, M. F., Sotiropoulos, S. N., Wilson, J. A., Coalson, T. S., Fischl, B., Andersson, J. L., ... WU-Minn HCP Consortium. (2013). The minimal preprocessing pipelines for the human connectome project. *NeuroImage*, 80, 105–124.
- Griffa, A., Baumann, P. S., Thiran, J.-P., & Hagmann, P. (2013). Structural connectomics in brain diseases. *NeuroImage*, 80, 515–526.
- Hagmann, P., Cammoun, L., Gigandet, X., Meuli, R., Honey, C. J., Wedeen, V. J., & Sporns, O. (2008). Mapping the structural core of human cerebral cortex. *PLoS Biology*, 6, e159.
- Jones, D., Simmons, A., Williams, S., & Horsfield, M. (1998). Non-invasive assessment of structural connectivity in white matter by diffusion tensor MRI. Sixth annual meeting of the International Society for Magnetic Resonance in Medicine. Berkeley, CA: International Society for Magnetic Resonance in Medicine, p. 531.
- Maier-Hein, K. H., Neher, P. F., Houde, J.-C., Côté, M.-A., Garyfallidis, E., Zhong, J., ... Descoteaux, M. (2017). The challenge of mapping the human connectome based on diffusion tractography. *Nature Communications*, 8, 1349.
- Mandonnet, E., Sarubbo, S., & Petit, L. (2018). The nomenclature of human white matter association pathways: Proposal for a systematic taxonomic anatomical classification. *Frontiers in Neuroanatomy*, 12, 94.
- Meola, A., Comert, A., Yeh, F.-C., Stefanescu, L., & Fernandez-Miranda, J. C. (2015). The controversial existence of the human superior fronto-occipital fasciculus: Connectome-based tractographic study with microdissection validation. *Human Brain Mapping*, 36, 4964–4971.
- Mori, S., & van Zijl, P. (2002). Fiber tracking: Principles and strategies—a technical review. *NMR in Biomedicine*, 15, 468–480.
- Nathan, P., & Smith, M. C. (1955). Long descending tracts in man: I. Review of present knowledge. *Brain*, 78, 248–303.
- Pagnozzi, A. M., Conti, E., Calderoni, S., Fripp, J., & Rose, S. E. (2018). A systematic review of structural MRI biomarkers in autism spectrum disorder: A machine learning perspective. *International Journal of Developmental Neuroscience*, 71, 68–82.
- Panesar, S., & Fernandez-Miranda, J. (2019). Commentary: The nomenclature of human white matter association pathways: Proposal for a systematic taxonomic anatomical classification. *Frontiers in Neuroanatomy*, 13, 61.
- Rheault, F., De Benedictis, A., Daducci, A., Maffei, C., Tax, C. M., Romascano, D., ... Descoteaux, M. (2020). Tractostorm: The what,

- why, and how of tractography dissection reproducibility. *Human Brain Mapping*, 41, 1859–1874.
- Rheault, F., Houde, J.-C., Goyette, N., Morency, F., & Descoteaux, M. (2016). MI-brain, a software to handle tractograms and perform interactive virtual dissection. ISMRM diffusion study group workshop. Lisbon, Portugal.
- Rheault, F., Poulin, P., Caron, A. V., St-Onge, E., & Descoteaux, M. (2020). Common misconceptions, hidden biases and modern challenges of dMRI tractography. *Journal of Neural Engineering*, 17, 011001.
- Rosario, B. L., Weissfeld, L. A., Laymon, C. M., Mathis, C. A., Klunk, W. E., Berginc, M. D., ... Price, J. C. (2011). Inter-rater reliability of manual and automated region-of-interest delineation for PiB PET. *NeuroImage*, 55, 933–941.
- Schilling, K.G., Rheault, F., Petit, L., Hansen, C.B., Nath, V., Yeh, F.-C., ... Descoteaux, M. (2020). Tractography dissection variability: What happens when 42 groups dissect 14 white matter bundles on the same dataset? bioRxiv.
- Sefcikova, V., Sporrer, J. K., Ekert, J. O., Kirkman, M. A., & Samandouras, G. (2020). High interrater variability in intraoperative language testing and interpretation in awake brain mapping among neurosurgeons or neuropsychologists: An emerging need for standardization. *World Neurosurgery*, 141, e651–e660.
- Tournier, J.-D., Yeh, C.-H., Calamante, F., Cho, K.-H., Connelly, A., & Lin, C.-P. (2008). Resolving crossing fibres using constrained spherical deconvolution: Validation using diffusion-weighted imaging phantom data. *NeuroImage*, 42, 617–625.
- Türe, U., Yaşargil, M. G., & Pait, T. G. (1997). Is there a superior occipitofrontal fasciculus? A microsurgical anatomic study. *Neurosurgery*, 40, 1226–1232.
- Vavassori, L., Sarubbo, S., & Petit, L. (2021). Hodology of the superior longitudinal system of the human brain: A historical perspective, the current controversies, and a proposal. *Brain Structure & Function*, 226, 1363–1384.
- Visser, M., Müller, D., van Duijn, R., Smits, M., Verburg, N., Hendriks, E., ... de Munck, J. C. (2019). Inter-rater agreement in glioma segmentations on longitudinal MRI. *NeuroImage: Clinical*, 22, 101727.
- Wakana, S., Caprihan, A., Panzenboeck, M. M., Fallon, J. H., Perry, M., Gollub, R. L., ... Mori, S. (2007). Reproducibility of quantitative tractography methods applied to cerebral white matter. *NeuroImage*, 36, 630–644.
- Witelson, S. F. (1985). The brain connection: The corpus callosum is larger in left-handers. *Science*, 229, 665–668.
- Yeh, F.-C., Panesar, S., Fernandes, D., Meola, A., Yoshino, M., Fernandez-Miranda, J. C., ... Verstynen, T. (2018). Population-averaged atlas of the macroscale human structural connectome and its network topology. *NeuroImage*, 178, 57–68.

SUPPORTING INFORMATION

Additional supporting information may be found in the online version of the article at the publisher's website.

How to cite this article: Rheault, F., Schilling, K. G., Valcourt-Caron, A., Théberge, A., Poirier, C., Grenier, G., Guberman, G. I., Begnoche, J., Legarreta, J. H., Y. Cai, L., Roy, M., Edde, M., Caceres, M. P., Ocampo-Pineda, M., Al-Sharif, N., Karan, P., Bontempi, P., Obaid, S., Bosticardo, S., ... Landman, B. A. (2022). Tractostorm 2: Optimizing tractography dissection reproducibility with segmentation protocol dissemination. *Human Brain Mapping*, 1–14. <https://doi.org/10.1002/hbm.25777>

Variability evaluation of experts in human brain diffusion tractography

General instructions

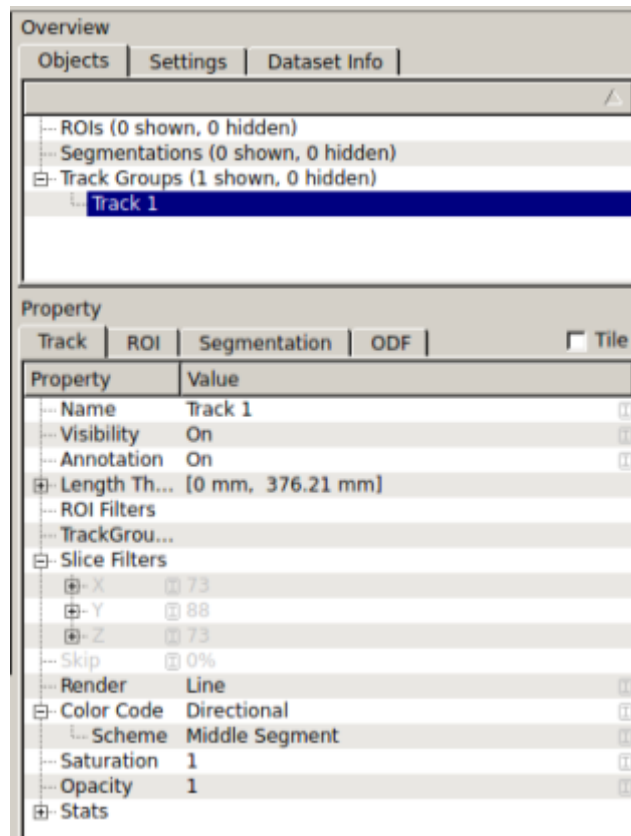
- The virtual manual dissections can only be performed with the software **TrackVis** (<http://trackvis.org/>) or **MI-Brain** (<https://www.imeka.ca/mi-brain>). Choose the software you are the most used to, please refrain from switching software unless necessary.
 - Usage of scripts to perform any steps of the segmentation automatically or semi-automatically is forbidden.
 - The tractograms were compressed to facilitate data sharing between organizers and participants.
 - Only drawn ROIs are allowed, these ROIs must be saved as nifti files. Do not use the disk, sphere or atlas option in trackvis or the cube, ellipse in MI-Brain.
- The dissection plan presented below is technically the same for both hemispheres, however only the left pyramidal tract and left arcuate fasciculus are required for this study.
 - The bundles of interest need to be segmented separately and saved as “PYT_L.trk”, “AF_L.trk” and “CC.trk” in the same folder as their associated subject.
 - To be optimal and facilitate analysis, the ROIs should be drawn in the same order as they are presented in the dissection plan. Please refrain from skipping ROIs during the protocol.
- The goal of this project is to study intra/inter participants’ variability. While staying within the limits of common sense, the amount of work for each dissection should be aimed at respecting the definition and maximize reproducibility. *(We suggest approximately 20 minutes per tractogram to dissect the 3 bundles)*
 - Perform the dissection in alphanumerical order and note the requested information in the spreadsheet (metadata).
 - Once a dissection is completed, please consider it final and do not edit previous subjects (except in major cases, please inform us if this happens).
 - We suggest “practice” on the first subject to familiarize with the dissection plan, the instructions and the software. When the participant is comfortable with the task, the second subject can be started.
- Others
 - Note that the size of ROI is mentioned in mm, the resolution of HCP datasets is 1.25mm isotropic. ($10mm/1.25mm = 8 \text{ voxels}$)
 - Any suggestions related to size of ROIs was based on the approximate size of landmark in a few datasets, the final decision should be based on the observed landmark in a dataset.
 - After each ROI is drawn, save it using the provided filename. Once all ROIs are saved, proceed with the final bundle segmentation.

- DON'T FORGET TO REMOVE **SKIP** OR **SLICE FILTERING** IN TRACKVIS

Trackvis skip and slice filtering options :

By default Trackvis is not showing all streamlines, which can affect your decision during the segmentation. Make sure to remove those options before doing any dissection.

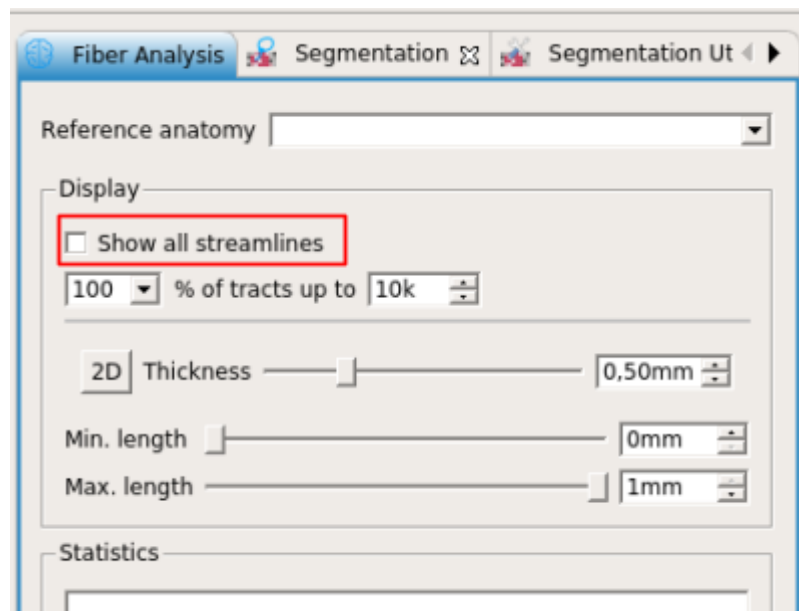
In the menu on the right, look for the Slice Filters and Skip option. By double clicking on the Y and the Skip you will see a checkbox appear. Uncheck it



DON'T FORGET TO CHECK **SHOW ALL STREAMLINES** IN MI-BRAIN

Show all streamlines option:

By default MI-Brain is not showing all streamlines, which can affect your decision during the segmentation. In the Fiber Analysis plugin view, simply check the option *Show all streamlines*

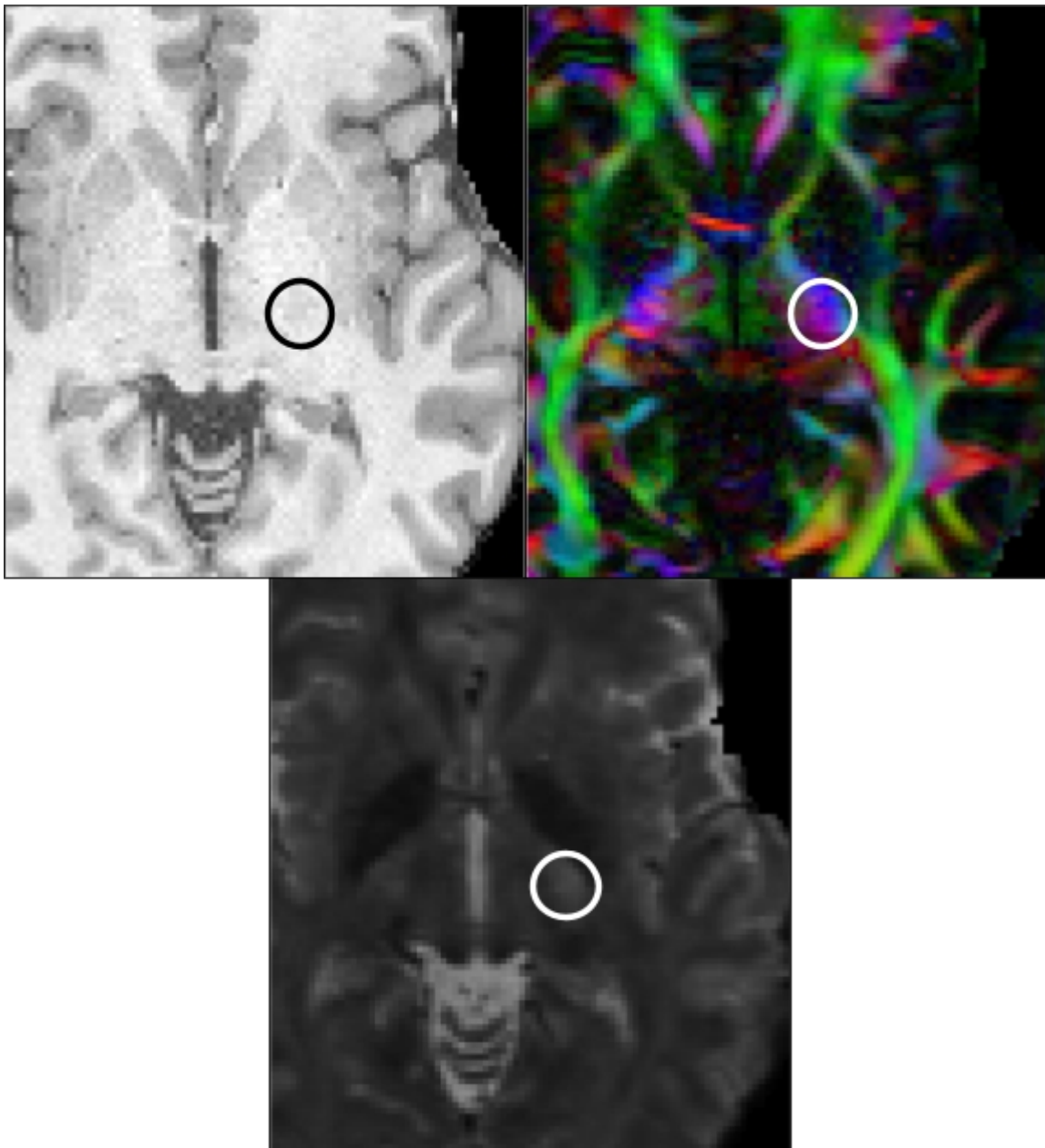


Instructions for the virtual dissection of the Pyramidal Tract

Internal Capsule ROI (IC-ROI)

The IC-ROI is a disk with a diameter of 8-12mm delineated on a single axial slice. The position of this ROI in axial is the approximate barycenter of the thalamus as it nearly corresponds to the middle of the adjacent internal capsule. The IC-ROI is centered on the B0 hypersignal localized between the posterior part of the putamen and the thalamus, within the internal capsule. The same region is seen in blue on the RGB map, the IC-ROI needs to overlap on the hypersignal of the B0 and the blue signal of the RGB.

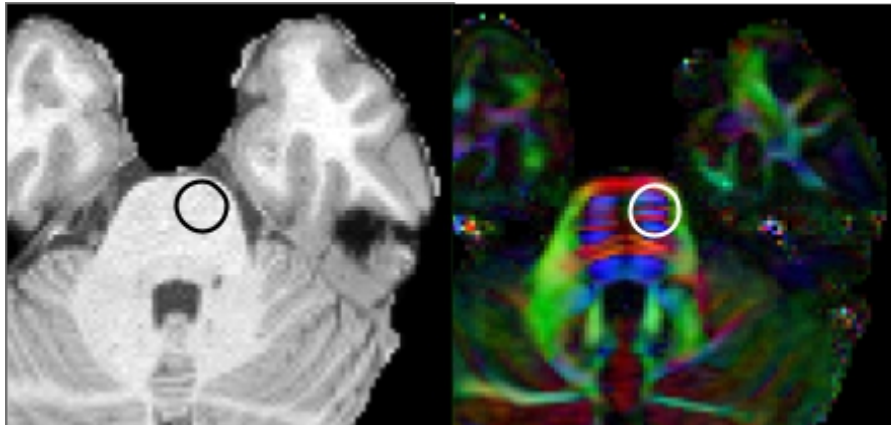
Save this ROI as IC_L.nii



Midbrain ROI (MB-ROI)

MB-ROI is a disk with a diameter of 12-16mm delineated on a single axial slice. It is used to discriminate the PyT (motor pathway) localized in the anterior part of the midbrain from the lemniscus tract (sensory pathway) localized in the posterior part of the midbrain. To position this ROI on axial slice, the RGB color map is used to highlight both tracts in blue color. The axial section in which the two tracts are the most distant from each other is then selected, and the ROI need to be centered on the blue signal located in the anterior part of the midbrain.

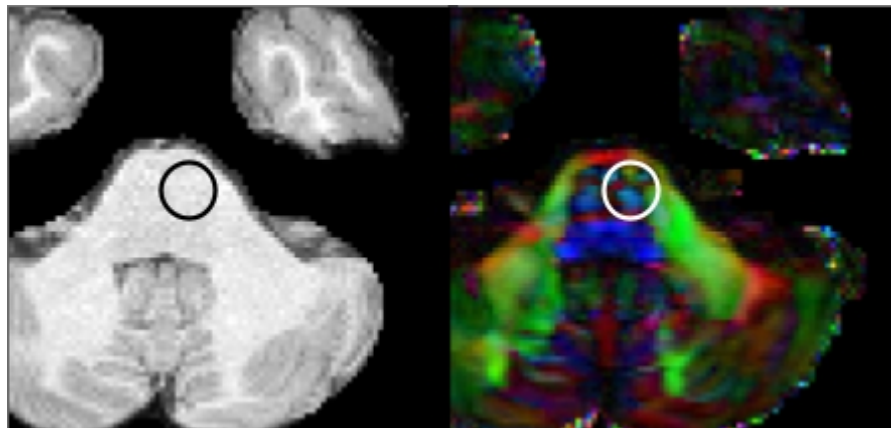
Save this ROI as MB_L.nii



Pyramids of the Medulla Oblongata (MO-ROI)

MO-ROI is a disk with a diameter of 10-14mm delineated on a single axial slice, which is used to select fibers entering in the medulla while not passing through the cerebellum. Note that at this level, the fibers are forming a pyramidal section. To position the MO-ROI in axial, the T1 and RGB color map are used at the level of the medulla oblongata. The criterion of selection is that the white matter of the medulla oblongata (rather in blue) has to be separated from the white matter of the cerebellum (rather in green) and had to form a pyramidal section in the T1 map when varying the grey-scale. The ROI then needs to be centered on the blue signal located in the anterior part of the Medulla Oblongata.

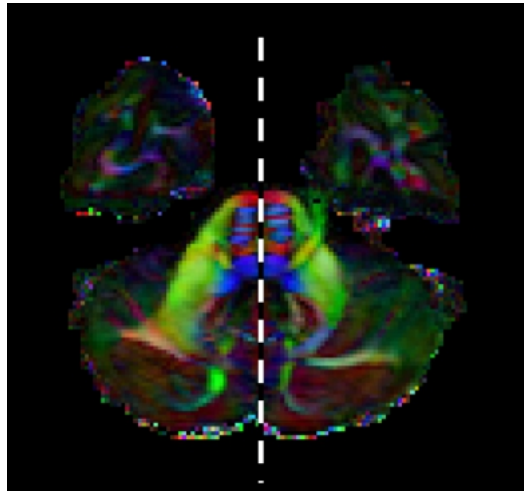
Save this ROI as MO_L.nii



Mid-sagittal plane cleaning

To prevent any contamination from implausible commissural streamlines, an extra mid-sagittal plane must be added. Create a planar sagittal ROI on the whole volume at the interhemispheric fissure. Be sure to verify the brainstem in order not to cut the pathway where the pyramidal tract is expected to go through, move the plan to the left to avoid this situation.

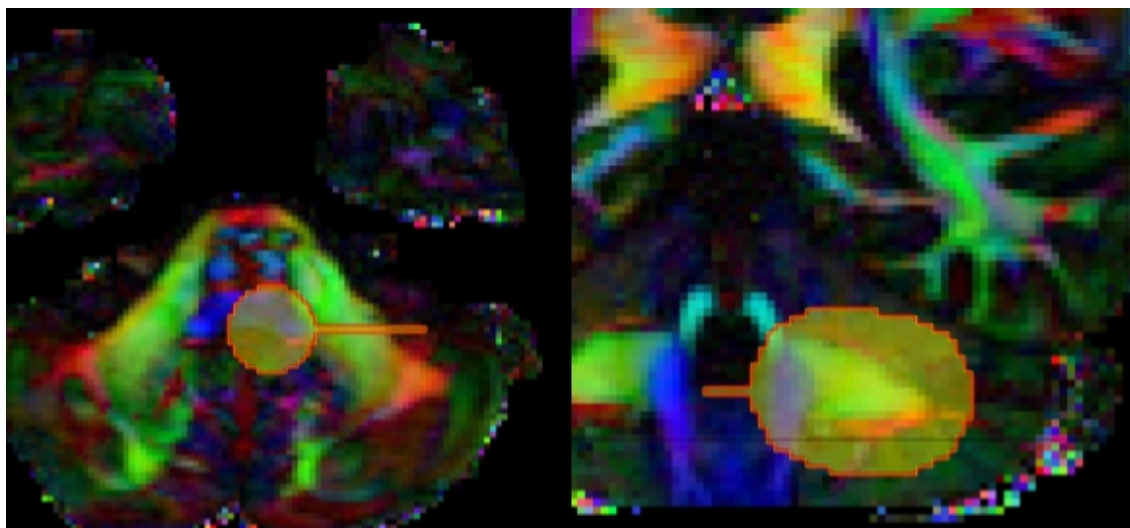
Save this as one ROI named MID_SAGITTAL_PLANE.nii



Cerebellum cleaning

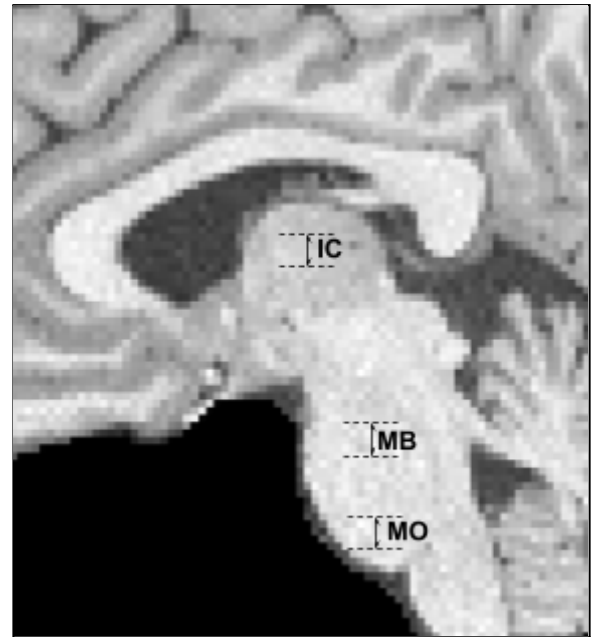
Spurious streamlines entering the cerebellum can be cleaned using two planar ROIs. One the same axial slice as the MO-ROI, place a much larger ROI (around 15-20mm) to prevent streamlines from using the wrong pathway (going behind the pyramid instead of going through it). The second ROI is a coronal plane placed behind the medulla oblongata ROI of size around 15-20mm. This ROI should cut off the entrance of the cerebellar peduncle without affecting the streamlines reaching down to the spinal cord. The result of this operation should be two intersecting disks with an offset of their center in the x-axis.

Save this as one ROI named MO_L_NOT.nii



How to easily locate these ROIs

For those with difficulties to locate the approximate position of the 3 previous ROIs, these small intervals should help to locate the landmarks described above. These are approximate positions to facilitate the initial search if you are not familiar with the anatomical structures used in the description. (see example)



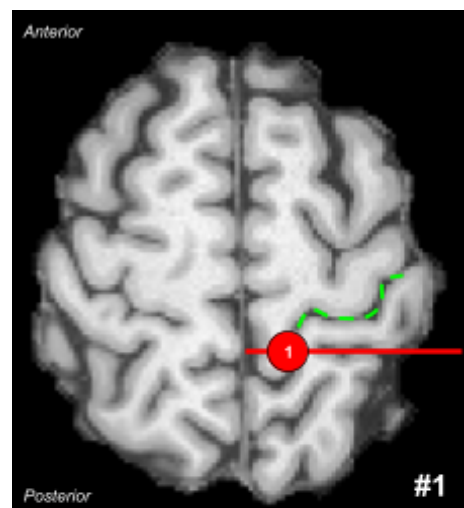
Precentral and postcentral ROIs

The bundle of interest should be restricted to termination within the precentral or postcentral gyri. Exclusion ROIs (covering two coronal slices) must be placed anterior to the precentral gyrus and posterior to the postcentral gyrus to avoid the superior part of the PyT from projecting too much anteriorly or posteriorly (see example).

1. Use the T1 in the axial plane to locate the Rolando sulcus (green line in figure #1), known as the deepest (most medial termination) sulcus seen on the axial slice and that includes the omega shape of the motor hand area, namely the genu of Rolando. The gyrus immediately posterior the Rolando sulcus is the postcentral gyrus while the immediately anterior one is the precentral gyrus.

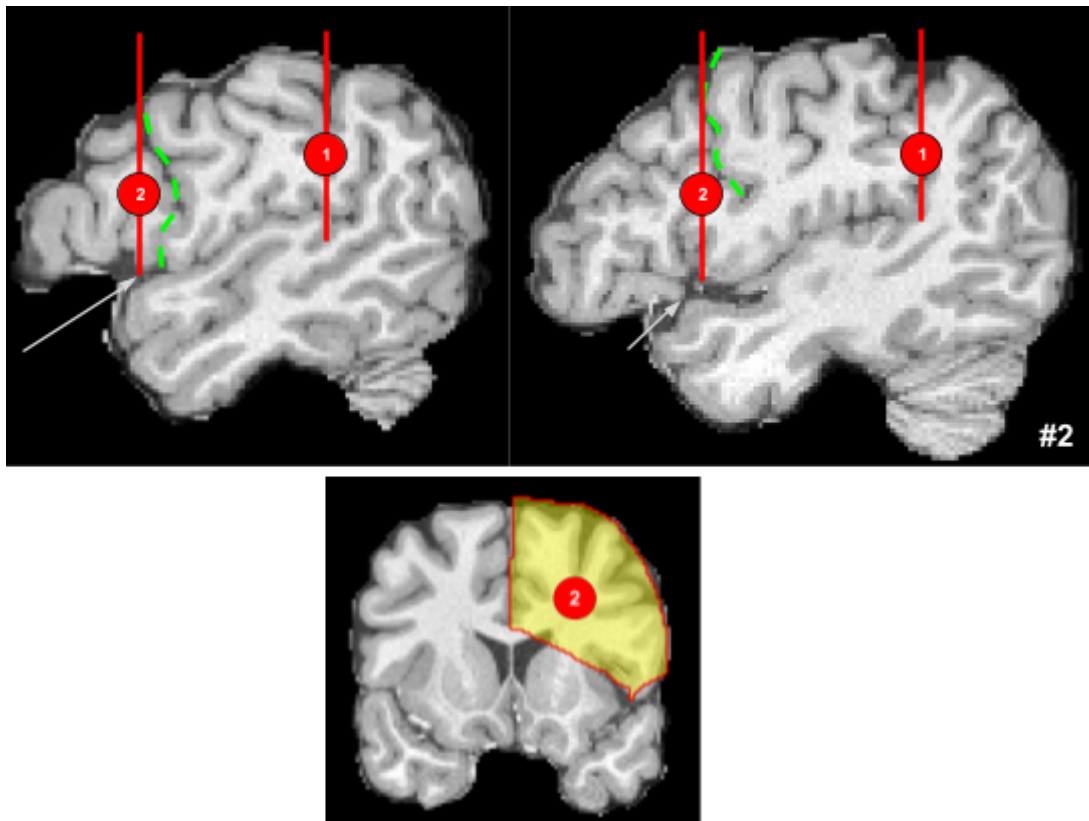
The first coronal planar exclusion ROI is then placed at the most posterior portion of the postcentral gyrus, at the level of the postcentral sulcus (red line 1).

Save the postcentral gyrus ROI (1) as POST_C_L.nii



2. The second coronal planar exclusion ROI is placed at the most anterior portion of the precentral gyrus, at the level of the precentral sulcus (red line 2). Use the T1 in the sagittal incidence to find the approximate region where the sylvian fissure starts. From the surface of the T1, scroll medially until you see the fissure, the lateral sulcus divides both the frontal lobe and temporal lobe.

Above that point, you should see the precentral gyrus generally following the Z axis. You may have to look at more than one sagittal slice to find the gyrus.



It is important not to cut the brainstem in the plane for the postcentral gyrus (1) and not to include nuclei in the plane for the precentral gyrus (2). The inclusion of the temporal lobe in postcentral gyrus ROI (1) is important as it will be used later for the arcuate fasciculus segmentation. The exclusion of the nuclei and temporal stem in the precentral gyrus ROI is important as it will be used later for the arcuate fasciculus segmentation.

Save the precentral gyrus ROI (2) as PRE_C_L.nii.

These ROIs must be segmented on the right side too (POST_C_R.nii and PRE_C_R.nii), they will be required later for the corpus callosum segmentation.

Instructions for the virtual dissection of the Corpus Callosum

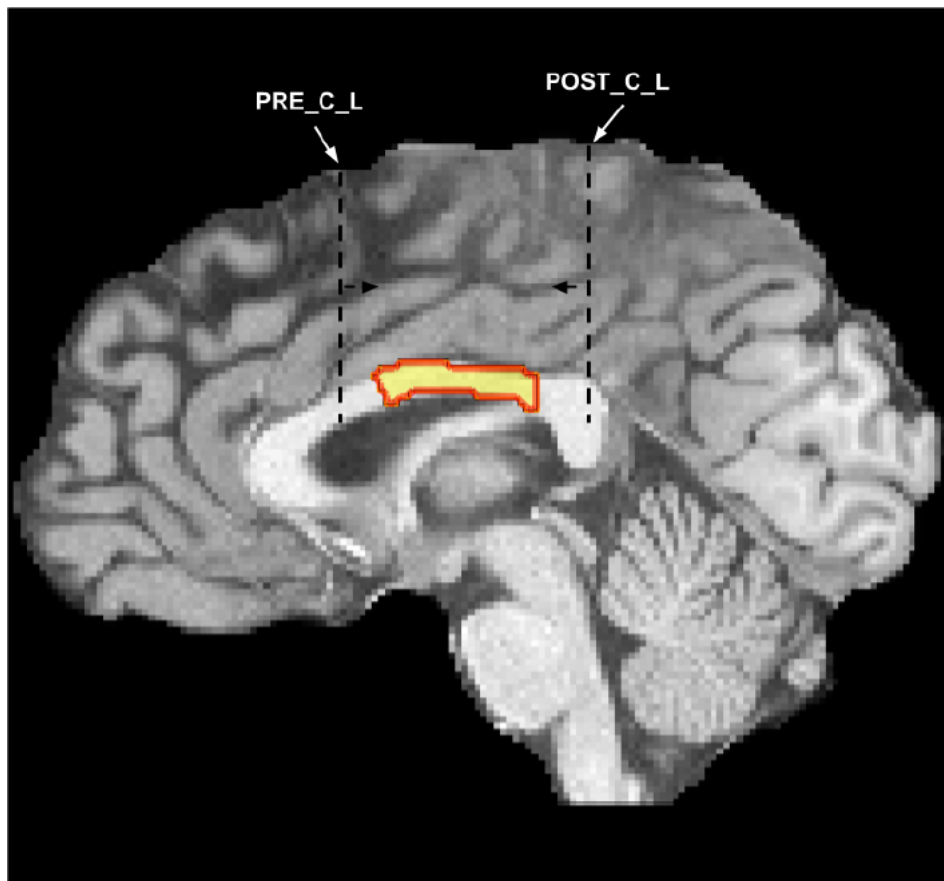
Central Corpus Callosum ROI (CCC-ROI)

In order to restrict the corpus callosum segmentation to the precentral and postcentral gyrus, a ROI must be added in the mid-sagittal plane. This ROI approximates the mid-anterior, central and mid-posterior region of the CC. However, this is in fact done solely to exclude the genu, the anterior portion of the CC and the splenium.

On the T1w image, from the center between the precentral gyrus and the postcentral gyrus (defined above), draw a 20-30mm long square region. This region should not have any curvature and should stop before the precentral gyrus and the postcentral gyrus planes.

The precentral gyrus and postcentral gyrus in both hemispheres (described above) are necessary to restrict the corpus callosum terminations.

Save this ROI as CENTRAL_CC.nii

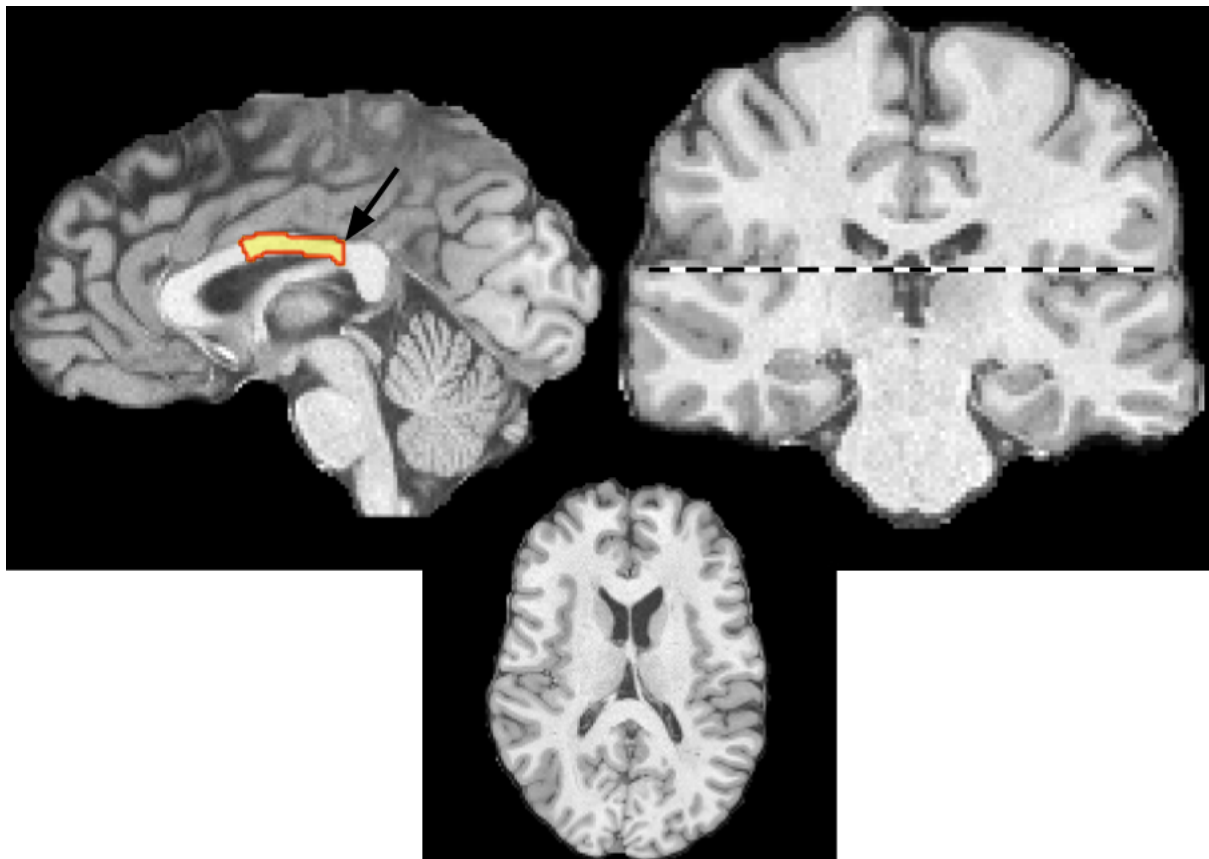


Lower limit of the Corpus Callosum (LOW-ROI)

To prevent streamlines from reaching into the nuclei, a planar axial exclusion ROI must be added. Using the most posterior position of the CCC-ROI as a coronal landmark (described above). Create a planar sagittal ROI on the whole volume just below the ventricle (or the sylvian fissure, whichever is lower).

This plane is used to approximate the position of the nuclei below the central corpus callosum as well as preventing the most posterior streamlines to curve into the temporal lobe following the tapetum.

Save this ROI as LOWER_AXIAL_LIM.nii

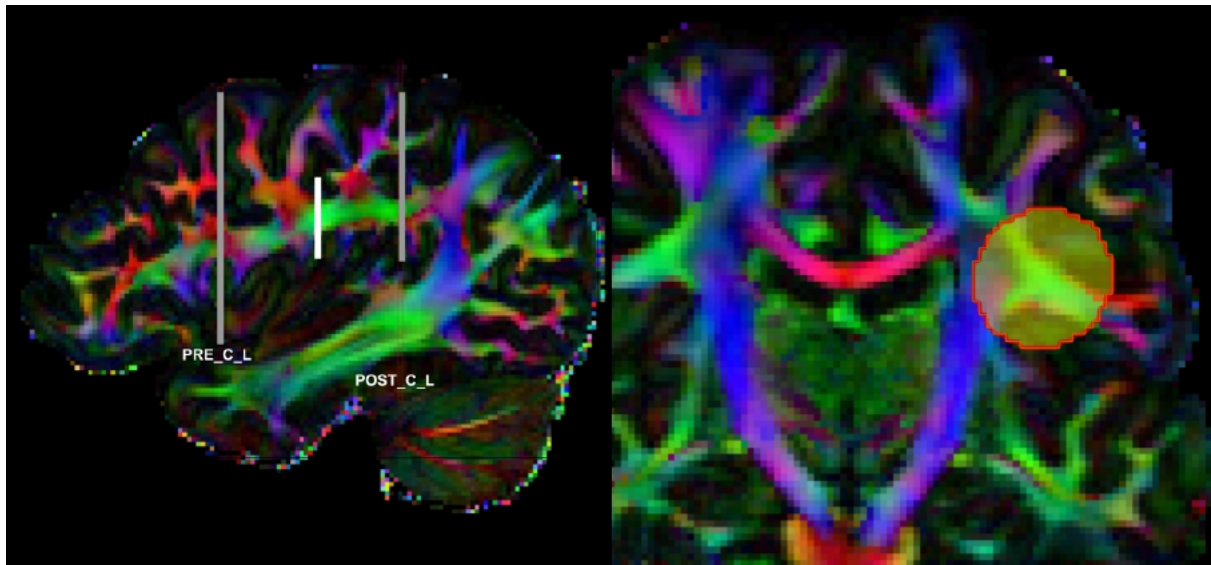


Instructions for the virtual dissection of the Arcuate Fasciculus

Centrum semiovale ROI (CS-ROI)

The CS-ROI is a disk/square with a diameter of 15-20mm delineated on a single coronal slice. The approximate center between the precentral gyrus and the postcentral gyrus (defined above) is used as a coronal landmark. The CS-ROI is centered on the green signal from the RGB map. This region approximates the core/stem of the dorsal pathways in the centrum semiovale. The green signal to locate is triangular in shape and should not extend into the core/stem of the superior longitudinal fasciculus I/II.

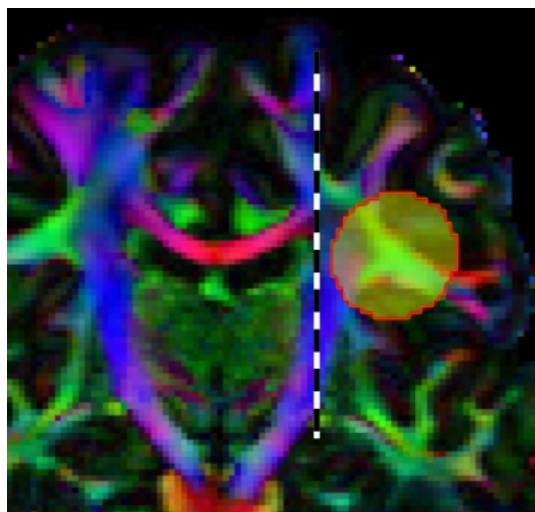
Save this ROI as CENTRAL_CS_L.nii



Medial limit of the Arcuate Fasciculus

The medial limit of the arcuate fasciculus can be approximated using a planar sagittal exclusion ROI estimated from the same slice as the CS-ROI. At the most medial position of the green signal on the RGB map, create a planar sagittal ROI on the whole volume.

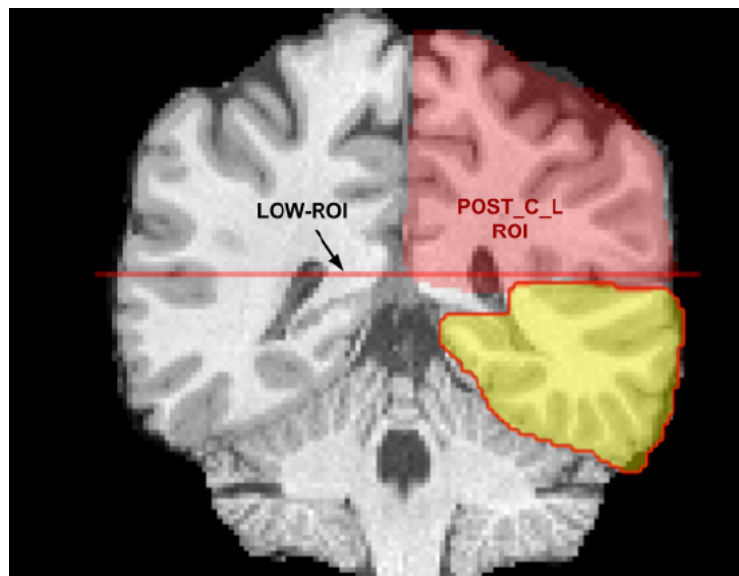
Save this ROI as MEDIAL_SAGITTAL_LIM.nii



Temporal lobe entrance ROI (TEMP-ROI)

The TEMP-ROI should approximate the entrance to the temporal lobe. On the same coronal slice as the postcentral gyrus ROI (described above, PyT), below the lower axial limit ROI (describe above, CC), draw a large square/circle ROI of approximately 25-35mm to encompass the temporal lobe.

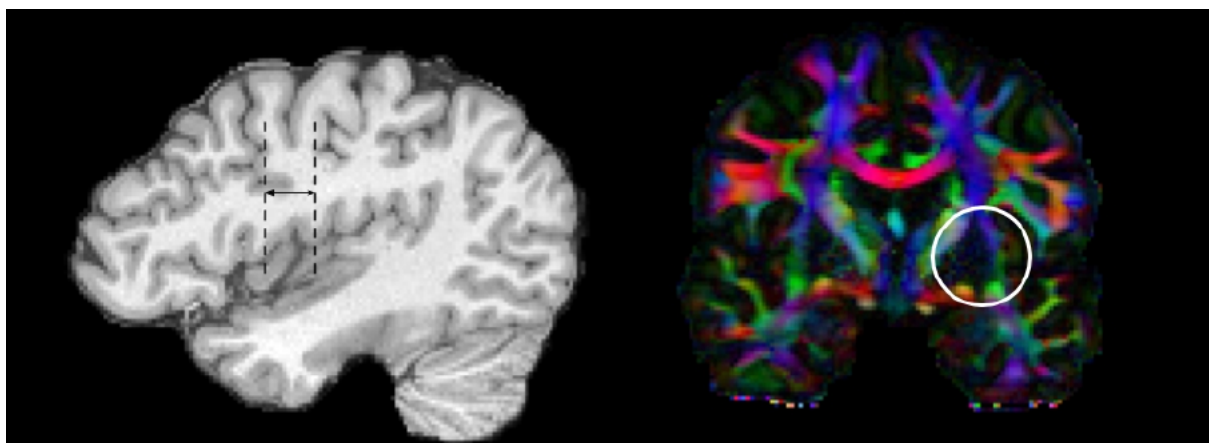
Save this ROI as TEMPORAL_ENTRY.nii



Temporal stem entrance ROI (STEM-ROI)

To prevent streamlines from reaching into the temporal stem, a disk/square coronal exclusion ROI must be added. Using the sylvian fissure, just behind the precentral gyrus (described above) as a coronal landmark, draw a disk/square of approximately 20-25mm encompassing the green signal in the RGB in its lower portion. The ROI should not cut into the main stem/core of the AF passing through the centrum semiovale. This ROI will be used to remove streamlines entering the temporal lobe via the temporal stem (part of the uncinate fasciculus).

Save this ROI as TEMPORAL_STEM.nii



Overview of the files and segmentation

After the segmentation, 15 files should have been saved. Only 2 files are related to the right hemisphere. The results of each segmentation must be saved separately, meaning that three tractography files (**TRK**) must be saved.

An example of the files, ROIs and bundles, is provided as a demonstration of the approximate expectation from this protocol. It should not be interpreted as perfect, only to help visualize the shape and position of what is asked. They represent the expected results of the dissection plan. This should help the non-experts among the participants.

Pyramidal Tract left (PYT_L.trk)

IC_L.nii	inclusion	small
MB_L.nii	inclusion	small
MO_L.nii	inclusion	small
MO_L_NOT.nii	exclusion	large
PRE_C_L.nii	exclusion	large
POST_C_L.nii	exclusion	large
MID_SAGITTAL_PLANE.nii	exclusion	plane

Arcuate Fasciculus left (AF_L.trk)

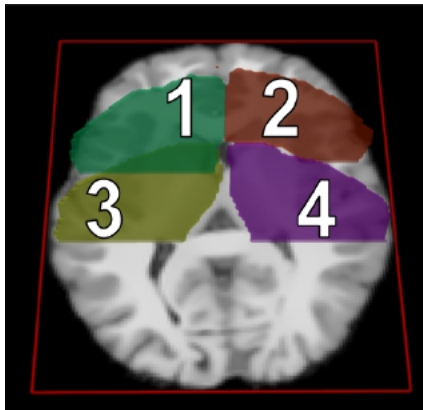
CENTRAL_CS.nii	inclusion	small
PRE_C_L.nii	inclusion	large
POST_C_L.nii	inclusion	large
TEMPORAL_ENTRY.nii	inclusion	large
TEMPORAL_STEM.nii	exclusion	large
MEDIAL_SAGITTAL_LIM.nii	exclusion	plane

Central Corpus Callosum (CC.trk)

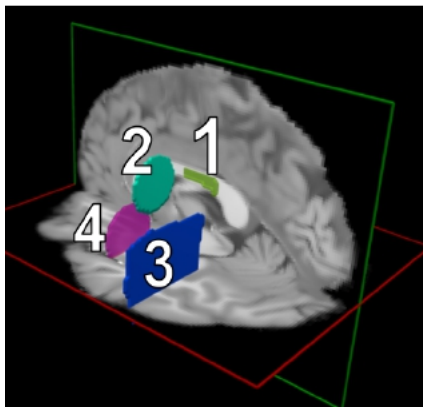
CENTRAL_CC.nii	inclusion	small
PRE_C_L.nii	exclusion	large
POST_C_L.nii	exclusion	large
PRE_C_R.nii	exclusion	large
POST_C_R.nii	exclusion	large
LOWER_AXIAL_LIM.nii	exclusion	plane

Approximate location of the ROIs

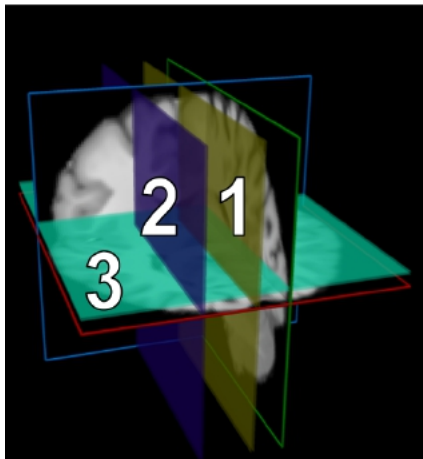
The ROIs are shown here in 3D and associated with their expected filename. Please follow the main description, this should be used only as an *aide-memoire*. (See example files)



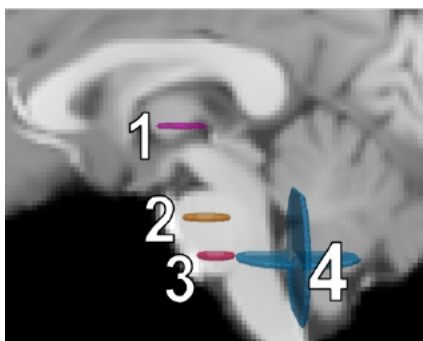
1. PRE_C_L
2. PRE_C_R
3. POST_C_L
4. POST_C_R



1. CENTRAL_CC
2. CENTRAL_CS
3. TEMPORAL_ENTRY
4. TEMPORAL_STEM



1. MID_SAGITTAL_PLANE
2. MEDIAL_SAGITTAL_LIM
3. LOW_AXIAL_LIM

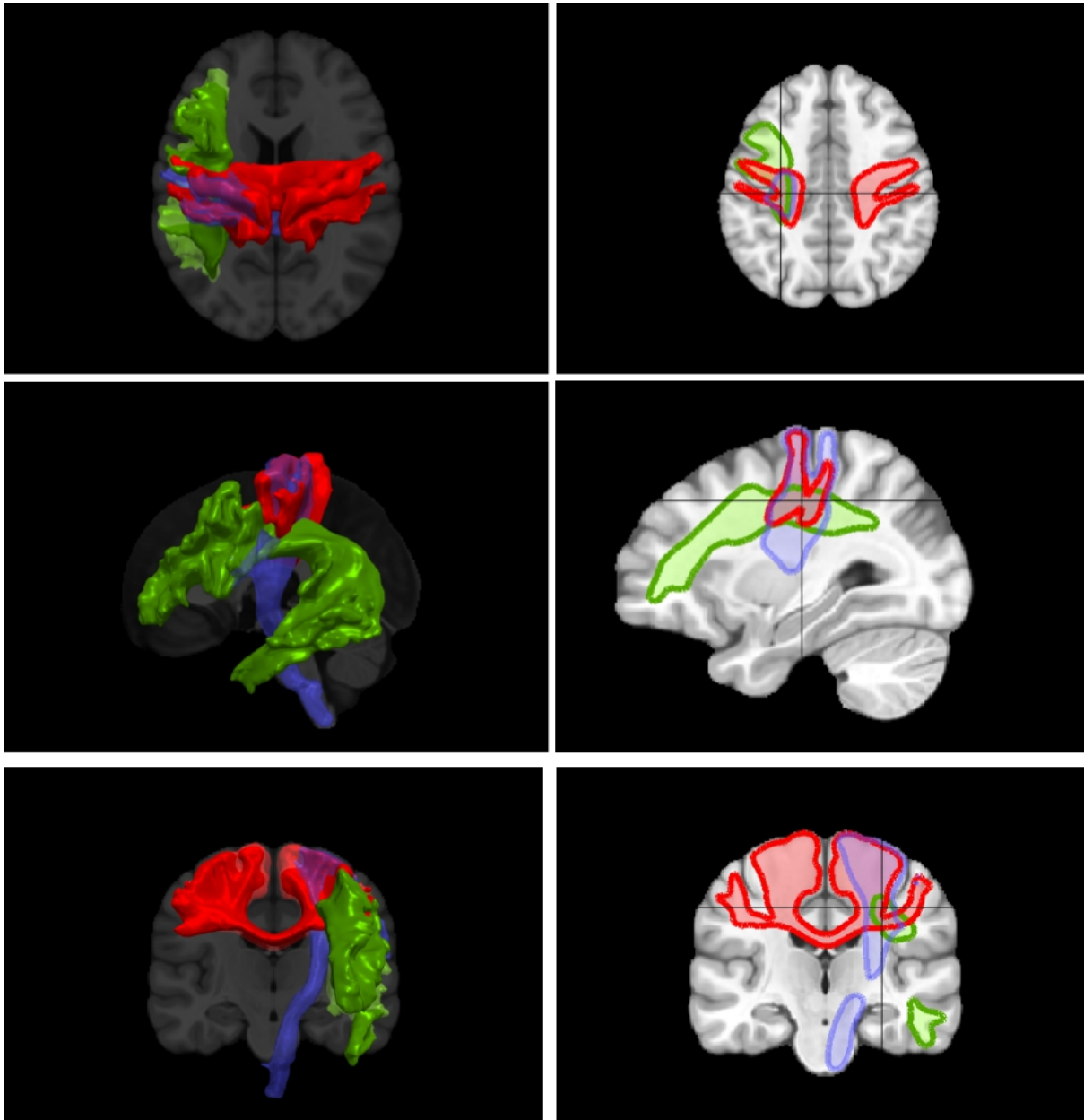


1. IC_L
2. MB_L
3. MO_L
4. MO_L_NOT

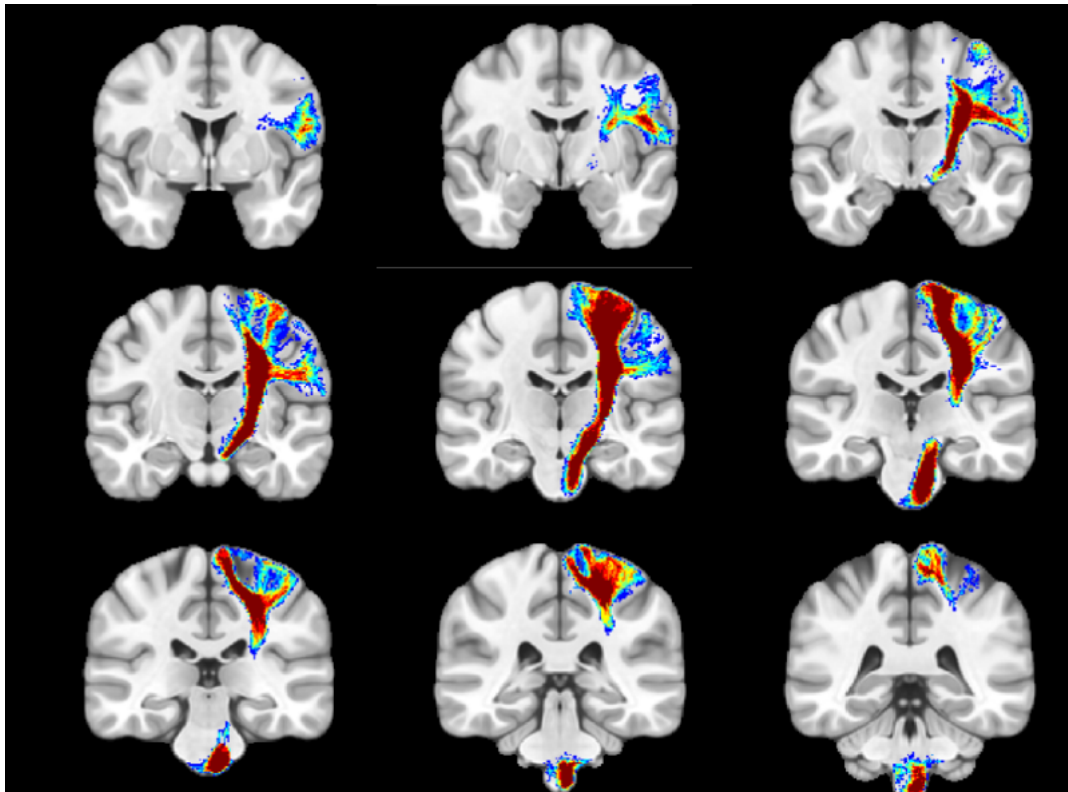
Average position/shape of bundles

Based on a small sample (10) of HCP datasets registered to MNI space, this is the expected position and shape of the bundle presented in this document. This should be used only as a way to easily orient yourself in the provided dataset. Furthermore, any results with a drastic difference from these shapes should be investigated as a potential error resulting from using the wrong segmentation rules or misnaming ROIs.

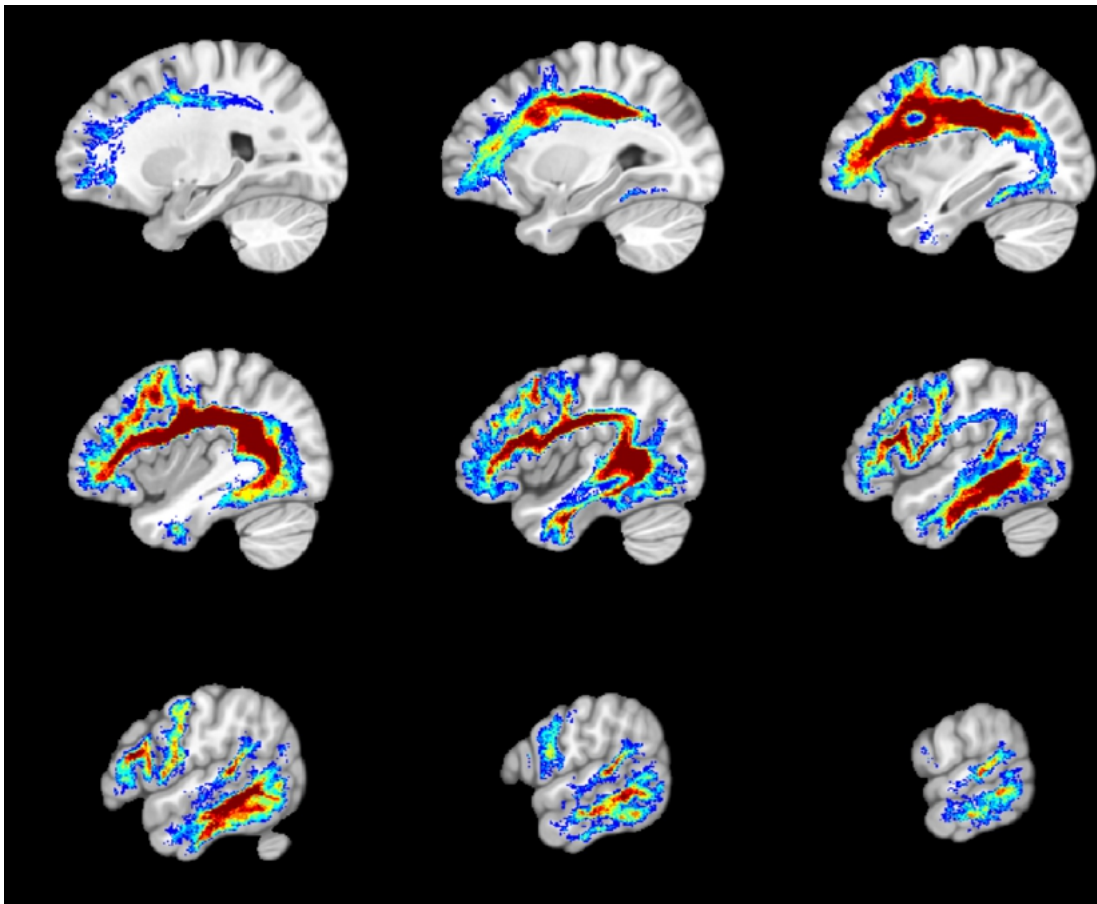
Isosurface at the probability value of 0.5.



Coronal mosaic of the probability value over a population of 10 for the pyramidal tract left.



Sagittal mosaic of the probability value over a population of 10 for the arcuate fasciculus.



Coronal mosaic of the probability value over a population of 10 for the corpus callosum.

